Motional Feedback in a Bass Loudspeaker

Analogue Implementation

by

Ivo van Straalen & Vyasa Krishnasing

TUDelft
Delft
University of
Technology

Preface

First and foremost we would like tot thank Dr.ir. G.J.M. Janssen, our supervisor, for giving us the proper guidance and sporadically putting us on the right track. Also we would like to thank the Tellegen Hall team for the resources and patience and those whom provided advice. Our interest in this field grew throughout this project. Hence it was disappointing that no tests on the loudspeaker could have been done yet. This will probably be done in the next few weeks, however.

Ivo van Straalen & Vyasa Krishnasing
Delft, June 2018

Abstract

This thesis is part of the Bachelor Graduation Project of Electrical Engineering at Delft University of Technology. This contains the complete design process of an analogue implementation of a Motional Feedback controller. Although the complete controller has been designed, no significant test results have yet been acquired. However, theoretically the linear distortion at $20\,Hz$ is reduced by 99.88% by the controller. Also is predicted that the nonlinear distortion is suppressed, because of the high loop gain. The feedback signal is generated using an accelerometer. The controller mainly consists of a PI-controller and a predistortion filter by means of a Linkwitz Transform.

Contents

1

Introduction

A loudspeaker, like any real electro-mechanical transducer, is a non-ideal device with physical properties and limitations. At low signal amplitudes, where its behaviour can be approximated as linear, the speaker manifests distortion of the input signal in the form of a non-flat transfer function. At high excursions of the cone and especially when reproducing lower frequencies where high amplitudes are needed to generate the same audio power, non-linearities in the electrical and mechanical properties of the speaker cause additional deformation of the sound in the form of audible harmonic and intermodulation distortion.

One way to reduce the detrimental effects of both the linear and non-linear behaviour of the speaker is by using negative feedback to correct for this distortion. Some sources of feedback signals that have been used are the back EMF of the speaker voice coil [1] and that of a secondary voice coil mounted on the diaphragm [2], but these methods are not sufficient to produce the best possible results.

In 1968, a motional feedback system was proposed by Philips [3] to suppress linear and non-linear distortion in bass speakers. The system used a piezoelectric accelerometer mounted on the speaker cone to measure its acceleration. The recorded signal was fed back to a control system which compensated for the distortion and improved the performance of the speaker.

The concept of Motional Feedback will be studied and applied as our Bachelor's Graduation Project. The team working on this project consists of three sub-groups each working on a different implementation of this concept, namely: the analogue, digital and theory group. It is meant that the digital group will try to come up with a digital implementation of this motional feedback controller. The analogue group is expected to design an analogue implementation of this system. The theory group will parametrise the speaker in order to create a model of the non-linear loudspeaker and work towards designing an optimal controller. This model as well as the measurement setup and code used to measure the performance of the speaker will be used to validate the controller designed by the other two subgroups. This thesis will cover the analogue part.

What is expected from this project is thoroughly explained in Section 1.1. A profound theoretical description of a generic loudspeaker and description of the problems the speaker is currently suffering from will be discussed in Section 2. Next the complete step-by-step description of the design process will be discussed in Section 3. Then the test procedure will be discussed ending with a discussion and conclusion.

1.1. Programme of Requirements

The products to be developed are an analogue and a digital implementation of a motional feedback system for a bass loudspeaker using the feedback signal of a piezo-electric accelerometer mounted on the speaker cone, as well as a theoretical model of a loudspeaker and motional feedback controller. The system is a low-cost, small format implementation which can easily be adjusted to be used for different speakers

1

with different characteristics. The system is aimed towards commercial loudspeaker manufacturers to be included in active loudspeaker systems. The consumer good must meet or improve on the specifications listed in Section 1.1.1 when using motional feedback and. It also has to be available for a lower price than other motional feedback loudspeaker systems with similar specifications available on the market.

1.1.1. Requirement formulation

1. **MR:** mandatory requirements

   - A woofer loudspeaker diaphragm is equipped with a piezo-electric accelerometer. The signal thereof is to be included in a negative feedback loop; this principle is known as Motional Feedback (MFB).
   - The system should operate in a bandwidth from $10 - 300 Hz$, however, a $1 kHz$ bandwidth is highly desirable. The highest attainable bandwidth is $2 kHz$ due to sensor limitations.
   - The cost of the system should be no more than € 100.
   - The volume of the controller should be 0.5 L maximum.
   - The Total Harmonic Distortion (THD) should be reduced to 0.1%.
   - The largest acceptable delay that is introduced as a result of the controller is 120 ms. This is the delay that the user may experience when playing sound through the system.
   - The power consumption of the controller should be 100 mW.
   - The theoretical model of the loudspeaker must be accurate enough that the relative error in the simulated and measured Total HD is not larger than 1% in the bandwidth stated above.

2. **ToRs:** Trade-off requirements

   - The desired Signal to Noise Ratio (SNR) is at least 100 dB. Nevertheless, a 16 bit digital system may offer some advantages due to faster communication possibilities and lower cost. The SNR of a 16 bit system is at most 80 dB, but this acceptable also..
   - The system is optimised for the specific loudspeaker and amplifier that have been made available for this project. The system should ideally be also applicable to other configurations, considering the typical amplifier gain is $20 - 30$ dB.
   - The system must be stable, which implies that both the gain and phase margins must be reasonable. Precise minima were not given, but a phase margin of 45 degrees was proposed, alongside a gain margin of 3 dB.

1.1.2. Study-case

1. **Functional Requirements**

   (a) The MFB system must operate whenever the loudspeaker system is turned on without requiring additional steps from the user.

   (b) The loudspeaker system's user interface may contain a switch to turn motional feedback on and off.

2. **System Requirements**

   (a) **Utilisation features**

      i. The lifespan of the feedback controller and accelerometer must be at least as long as the lifespan of the loudspeakers in which it is included.

      ii. If support and/or maintenance is provided for the loudspeaker system, this must include support for the MFB system.

   (b) **Production and putting into use features**

      i. Inclusion of the MFB system must take place during the development of the loudspeaker system in cooperation between the loudspeaker manufacturer and the company implementing motional feedback.

     ii. The loudspeaker must undergo testing by the company before and after the inclusion of the MFB system to ensure MFB meets performance specifications.

    iii. The company implementing motional feedback will provide the piezo-electric accelerometer and controller to the loudspeaker manufacturer. The manufacturer must install the MFB hardware into the consumer product during assembly. Placement of the controller inside the loudspeaker will be discussed with the manufacturer on a case by case basis.

(c) **Discarding features**

      i. If the hardware of the MFB system is enclosed in a casing, the casing must be made from recyclable materials.

     ii. In case the MFB system's lifespan exceeds that of the speaker itself, the manufacturer must provide to the consumer the option of returning the MFB hardware for use in a refurbished product.

3. **Development of manufacturing methodologies**

(a) The digital version of the MFB controller will be implemented as an ASIC.

(b) The ASIC must be adjustable after manufacturing to meet specifications in any loudspeakers in which it is included; Only one version of the ASIC will be developed and manufactured.

(c) The theoretical model of the loudspeaker and controller will be implemented in MATLAB and Simulink.

(d) A protocol and measurement setup will be developed for quick testing and validation of the loudspeaker system before and after the inclusion of MFB. Testing on a loudspeaker must not take longer than 20 minutes.

4. **Liquidation/recycling methodologies**

(a) At the end of the product's lifespan, the discarding thereof must comply to the norms referring to processing of small chemical waste.

5. **Business strategies, marketing an sales opportunities**

(a) The manufacturer of the loudspeaker must explicitly state the inclusion of the MFB feature on the packaging and documentation of the final product.

(b) the logo of the company implementing motional feedback must be included on the packaging and casing of the final product by the manufacturer.

2

Problem Definition

The following section describes a linear model for the loudspeaker as well as the cause and effects of nonlinearities that arise in the loudspeaker response. These are needed for both the design of the digital and analogue implementation, as well as being a foundation for the derivation of a nonlinear model and the design of the ideal controller.

2.1. Loudspeaker Model

A schematic of a generic loudspeaker can be seen in Figure 2.1. In short, it simply works by sending a current through the voice coil, which is then attracted or repelled by the permanent magnet. This causes the cone to move, which generates sound.
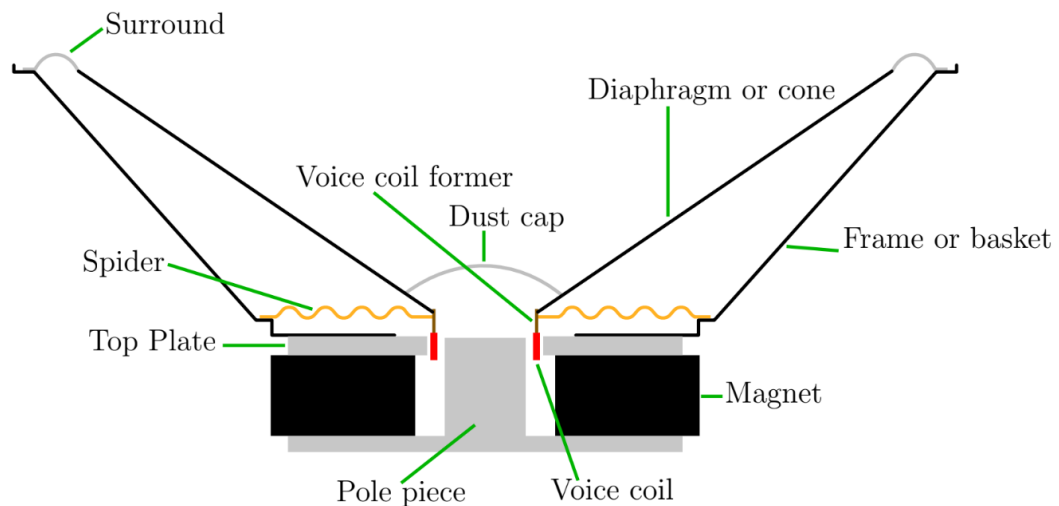

Figure 2.1: A cross-section of a typical loudspeaker. Courtesy of [4]

The electric, magnetic, mechanical and acoustic behaviour of the loudspeaker can be modelled using an electric circuit [5], which has the benefit of being able to calculate how the system reacts to an input signal. An example of such a circuit can be seen in Figure 2.2, in which an acoustic load has been neglected. The acoustic load can be neglected due to its very small magnitude [6]. This circuit only holds for low frequencies. However, since only a bass speaker is concerned, this constraint is no issue. The part of the circuit before the gyrator corresponds to the actual electrical part of the loudspeaker and that which comes after the gyrator corresponds to the mechanical components of the loudspeaker, hence the gyrator symbolises the transformation from the electrical domain to the mechanical domain with a factor $B \cdot l$. L_E
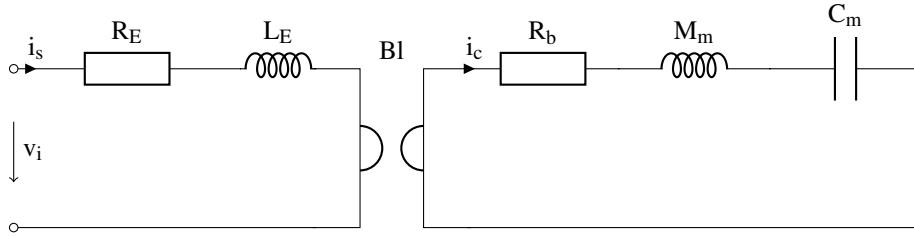
5

Figure 2.2: A schematic of the equivalent circuit for a loudspeaker. The left side of the gyrator represents the electrical domain, and the right side represents the mechanical domain.

is the selfinductance of the voice coil, R_E is its resistance and i_s is the current flowing through the voice coil. The current i_c is the electrical representation of the velocity of the cone, R_b represents the damping of the speaker cone, C_m represents the compliance of the speaker cone and M_m represents the mass of the moving speaker cone. The voltage across all the elements to the right of the gyrator represents the force acting upon the speaker cone.

From this simplified circuit a linear estimation of state-space model (see Equation 2.1) and a transfer function of the speaker can easily be derived, which can give a basic illustration of how the speaker behaves. But this was not used during the design process since determining the individual parameters of the speaker would take far too long. Also the derived transfer function will not provide a usable response, as the model only represents the impedance of the loudspeaker. However, the acoustic response of the loudspeaker is more important than the impedance when designing the controller. Thus instead the measured response will be used, this will be thoroughly discussed in Section 3.1.3.

$$\dot{\mathbf{x}} = \begin{bmatrix} \frac{-R_b}{R_m} & \frac{-1}{M_m \cdot C_m} & \frac{B \cdot l}{M_m} \\ 1 & 0 & 0 \\ \frac{-B \cdot l}{L_e} & 0 & \frac{-R_e}{L_e} \end{bmatrix} \mathbf{x} + \begin{bmatrix} 0 \\ 0 \\ \frac{1}{L_e(x)} \cdot v_i \end{bmatrix} \tag{2.1}$$

Where the vector $\mathbf{x}$ contains the state variables of the system, which are: $\dot{i}_c$, i_c and i_s. Which means the system is fully described by: i_s, the current through the voice coil, i_c, the velocity of the cone and $\dot{i}_c$, the acceleration of the cone.

2.2. Nonlinearities of a Loudspeaker

Loudspeakers in general tend tohave non-linear behaviour, especially at lower frequencies. These non-linear behaviours are caused by the physical limitations of such a transducer as well as the geometry and material properties of the loudspeaker components, several nonlinearities are present in the system. Most of these nonlinearities are prominent at higher amplitudes, and they can have detrimental effects on the quality of the sound produced. Klippel [3], Bai and Huang [4] give an overview of the main causes of nonlinearities in loudspeaker systems. The suspension, the force factor and the voice coil inductance are the main sources of these non-linearities and all depend on the displacement of the cone. This non-linear behaviour of the parameters affects the loudspeaker transfer at different frequencies inducing harmonic distortion. The subsequent sections will further elaborate separate sources of nonlinearty and the effect on the sound quality.

2.2.1. The suspension K_m

The stiffness of the suspension of a loudspeaker K_m is related to the mechanical properties of the two suspension components of the speaker cone: the spider and surround (Figure 2.1). For small displacements, K_m is constant and the suspension can be modelled as a linear spring. At higher displacements, the restoration force becomes larger as a function of x_d, the displacement of the cone, and a nonlinearity is introduced. The restoration force is given by:

$$F = K_m(x_d) x_d \tag{2.2}$$

The frequency dependency of the stiffness is linear. A related parameter to K_m is the compliance C_m, which is the inverse of the stiffness.
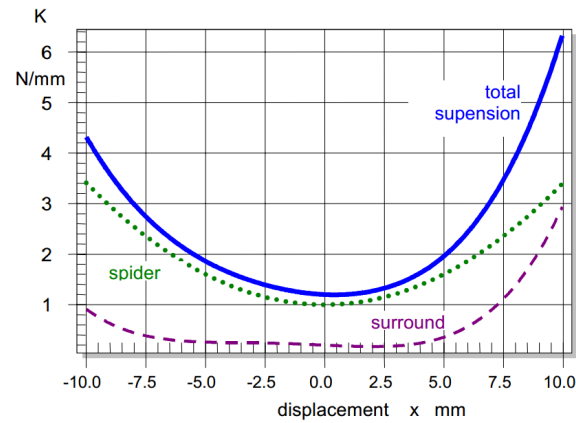

Figure 2.3: Force-Deflection curve showing nonlinearity of the spider and surround stiffness for large displacements.[7]

2.2.2. Force Factor $Bl(x_d)$

The force factor $Bl(x_d)$ is the integral of the flux density B over the effective wire length l of the voice coil in the air gap. It describes the coupling between the magnet and the voice coil of the loudspeaker. For a small displacement Bl is constant but for large displacement the voice coil leaves the gap and $Bl(x_d)$ decreases as function of displacement. This variation in the force factor introduces two nonlinearities:

- The back EMF u_{EMF} generated by the movement of the coil becomes dependent on displacement:

$$u_{EMF} = Bl(x_d)v \tag{2.3}$$

where v is the velocity of the speaker cone. This has the effect of variation in the electrical damping.

- The Lorentz force also becomes displacement dependent:

$$F = Bl(x_d)i \tag{2.4}$$

where i is the current in the voice coil. The force factor does not vary with frequency.
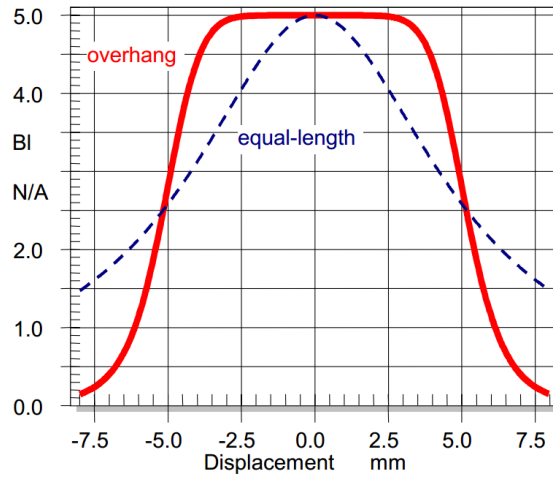
Figure 2.4: Plot showing non-linearity of the force factor for large displacements. The form of the Bl characteristic depends on the width of the voice coil, in the direction of movement, compared to the width of the gap. A coil which is wider than the gap will allow it to behave linearly for larger displacement.[7]

2.2.3. Voice Coil Inductance $L_E(x_d)$ and $L_E(i)$

The voice coil inductance L_E is also dependent on x_d. Because of the geometry of the loudspeaker motor, for positive displacement the magnetic field produced by the coil penetrates mainly the surrounding air, increasing magnetic reluctance thus decreasing the voice coil inductance. For negative displacement the magnetic field penetrates the steel surrounding the magnet (as well as the magnet) which has much higher permeability. This causes the reluctance to decrease and $L_E(x_d)$ to increase.

2.2.4. Harmonic and Intermodulation Distortion

In Figure 2.5, an arbitrary nonlinear function is shown, with the linearisation in the origin, which, in fact, according to [7], should resemble the restoration force that acts upon the loudspeaker cone. The slope of the graph is proportional to the suspension stiffness K_m, but its shape clearly indicates that it is dependent on the position x_d as well.

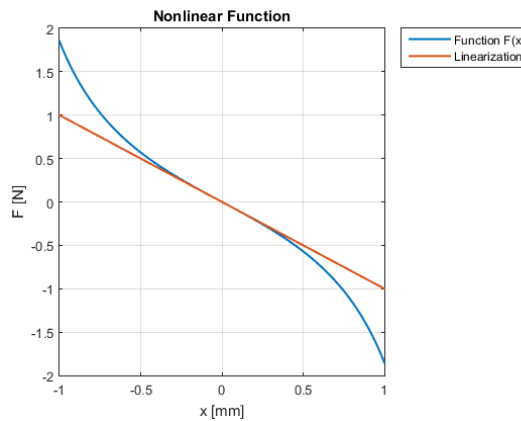Figure 2.5: Nonlinear function with linearised graph through the origin. The nonlinear function is a primitive model for the restoration force, which is related to the suspension stiffness $K_m(x_d)$.

The nonlinear function of Figure 2.5 can be expanded using Taylor expansion, which will give further insight in the distortion this will cause. The resulting expression is given in Equation 2.5. A third order

polynomial is used by [8] for the suspension stiffness. It is stated by [9] that a Gaussian sum may be the preferred choice over a polynomial expansion, because it is more accurate outside the initial range.

$$F(x_d) = a_0 + a_1 x_d + a_2 x_d^2 + a_3 x_d^3 + a_4 x_d^4 + a_5 x_d^5 \ldots \tag{2.5}$$

The offset term a_0 in the above equation is not of major concern, since it does not produce an audible frequency. Nevertheless, all terms except the a_1 term contribute to distortion. In order to understand the consequence of the higher order term, it is assumed that the nonlinear stiffness is an important contributor to distortion. As mentioned previously, this is the case below the resonance frequency. Thus, the output y of the system may be written as in Equation 2.6 as a function of the input i.

$$y = y_0 + \alpha_1 i + \alpha_2 i^2 + \alpha_3 i^3 + \alpha_4 i^4 + \alpha_5 i^5 + \ldots \tag{2.6}$$

It may be assumed that the input is sinusoidal function, e.g. $i = \cos \omega_0 t$. This assumption is very reasonable, since the input signal can be decomposed into an infinite set of sinusoids by the Fourier transform. The higher order terms α_n with $n \geq 2$ in Equation 2.6 will now generate harmonic distortion (HD). This can be understood by the notion that $i^2 = \cos^2(\omega_0 t) = \frac{1}{2} + \frac{1}{2} \cos(2\omega_0 t)$. The second order term therefore yields a spectral component with twice the frequency of the input signal. Table 2.1 gives an explicit expression for the powers of the input signal for $i = \cos(\omega_0 t)$ and the spectral components that are introduced.

Table 2.1: Explicit expression for i^n for $i = \cos(\omega_0 t)$. The spectral components that are generated by the higher order terms are listed. The frequency is given as $f = \frac{\omega}{2\pi}$ and DC corresponds to a frequency $f = 0$

n	i^n	spectral components
1	$\cos(\omega_0 t)$	f_0
2	$\frac{1}{2}\cos(2\omega_0 t) + \frac{1}{2}$	DC, $2f_0$
3	$\frac{1}{4}\cos(3\omega_0 t) + \frac{3}{4}\cos(\omega_0 t)$	$f_0, 3f_0$
4	$\frac{1}{8}\cos(4\omega_0 t) + \frac{1}{2}\cos(2\omega_0 t) + \frac{3}{8}$	DC, $2f_0, 4f_0$
5	$\frac{1}{16}\cos(5\omega_0 t) + \frac{5}{16}\cos(3\omega_0 t) + \frac{5}{8}\cos(\omega_0 t)$	$f_0, 3f_0, 5f_0$

As indicated in Table 2.1, the higher order terms introduce frequencies that are an integer multiple of the original frequency. These frequencies are commonly referred to as harmonics, hence the name harmonic distortion. It is suggested by [9] that harmonic distortion does not sound so bad. Unfortunately, the nonlinear system introduces another type of distortion known as intermodulation distortion (IMD) when two or more frequencies are played simultaneously. Supposing the input now consists of two sinusoids with the same amplitude, but different frequency: $i = \cos(\omega_0 t) + \cos(\omega_1 t)$. The second order term now yields: $i^2 = \cos((\omega_0 + \omega_1)t) + \cos((\omega_0 - \omega_1)t) + \cos^2(\omega_0 t) + \cos^2(\omega_1 t)$. The cosine squared terms produce harmonic distortion as seen before. However, additional spectral components with frequencies $(f_0 + f_1)$ and $|f_0 - f_1|$ are created also. These are the intermodulation frequencies, which may be perceived as unpleasant according to [9]. Table 2.2 lists the additional spectral components that are introduced for all nonzero order terms.

Table 2.2: Inter harmonic spectral components that are introduced by the i^n term of the nonlinear transfer, if the input is defined as: $i = \cos(\omega_0 t) + \cos(\omega_1 t)$.

n	spectral components
1	f_0, f_1
2	$f_0 + f_1, f_0 - f_1$
3	$2f_0 + f_1, 2f_0 - f_1, 2f_1 + f_0, 2f_1 - f_0$
4	$2f_0 + 2f_1, 2f_0 - 2f_1, 3f_0 + f_1, 3f_0 - f_1,$ $3f_1 + f_0, 3f_1 - f_0, f_0 + f_1, f_0 - f_1$
5	$4f_0 + f_1, 4f_0 - f_1, 4f_1 + f_0, 4f_1 - f_0,$ $3f_0 + 2f_1, 3f_0 - 2f_1, 3f_1 + 2f_0, 3f_1 - 2f_0,$ $2f_0 + f_1, 2f_0 - f_1, 2f_1 + f_0, 2f_1 - f_0$

Sixth or higher order terms in the nonlinear transfer may generate additional spectral components, but usually these components are quite small. In [10], the higher order spectral components can be seen, but they are below the measurement uncertainty and may therefore be neglected. In the measurements of e.g. [11], the third harmonic component is the most dominant. This implies that the odd terms of Equation 2.6 contribute significantly to the non-linearity. Intuitively, this means that the nonlinear function is more or less odd symmetric. It is stated in [7] that asymmetrical non-linearities generate primarily even-order distortion. It is also mentioned that even-order distortion is perceived as especially unpleasant. The graph in Figure 2.6 shows the frequency spectrum when distortion is introduced.
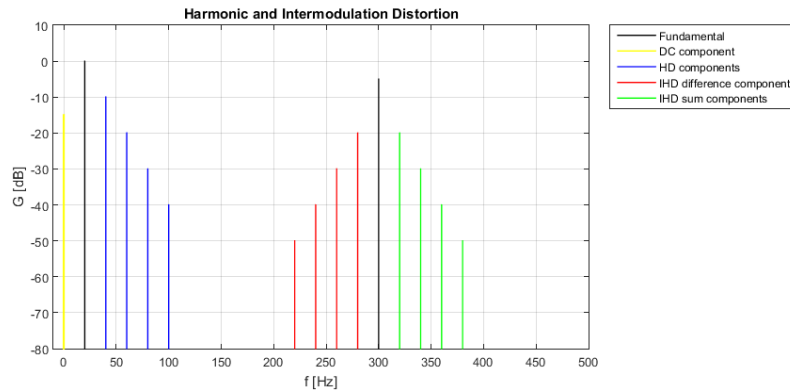

Figure 2.6: Frequency domain visualisation of harmonic (HD) and intermodulation distortion (IMD). Note that the frequency axis is linear. Additional spectral components may arise at higher frequencies, e.g. around 600 Hz but these are not indicated here.

2.3. Situation Assessment

Several solutions exist to tackle the phenomenon of distortion. The solution this project essentially uses is by means of a Motional Feedback controller (MFB). mentioned in the Introduction. Before designing any type of implementation of this MFB controller, it is needed to know about the past of this concept, what currently has been designed and what should still be done.

2.3.1. First developments

Phillips introduced motional feedback loudspeakers for the first time in 1968 [3]. The idea was to reduce the linear and non-linear distortion caused by a loudspeaker by including the loudspeaker in a feedback loop. Linear distortion is caused by the uneven distribution of intensity over the frequency spectrum (especially at lower frequencies) because the force needed to move the cone at low frequencies becomes larger. The nonlinear distortion generates higher harmonics. The radiated power was measured using an accelerometer attached to the cone and compared to the input voltage signal. Another advantage of motional feedback was that the speakers could be made smaller in volume without affecting the low frequency bass reproduction. The development of the motional feedback (MFB) loudspeakers was soon discontinued because it was too expensive at that time, to compete with conventional high-end loudspeakers [12]. MFB loudspeakers had excellent bass reproduction, however the overall tonal balance and cabinet coloration of the conventional loudspeakers was better. This was the first analogue implementation of the MFB-controller.

According to [13], feedback directly from the speaker cone can significantly reduce the distortion and improve the frequency response. With the use of a transducer (accelerometer) the direct output signal of the cone is negatively fed back to the input, but it is first pushed through a cascode stage. Directly working on the output of the speaker may have its benefits however, the transducer has a limited frequency range before it will no longer produce an accurate output (i.e it will introduce distortion at higher frequencies). This distortion can be filtered out by means of low-pass filtering, which in turn limits the use of motional-feedback to only low-frequency corrections. Luckily this concept was applied to a woofer. The transducer's bandwidth was limited to $44Hz$, because after this frequency the distortion of the transducer was higher than

the distortion of the woofer (at this frequency the distortion was around 0.5-1%). After applying motional feedback to the woofer significant distortion reduction was observed as well as the frequency response at lower frequency became more flat like.

In a later article by Philips [14], motional feedback using an accelerometer was also utilised. This time, also an amplifier circuit was designed. The feedback control again consists of a few stages. An impedance matching stage for correct reading of the accelerometer. This stage only consists of two resistors and a FET. Then a stage which takes care of maintaining the correct operating point of this FET and to relay the output signal for further processing. Then the final feedback stage consists of a filter-amplifier, which amplifies the signal such that it can be used as input for the main amplifier, as well as for making the feedback loop stable. This resulted in a flat frequency response for up t $130Hz$ lower than initially, and a reduction in the THD from 27% to 10% at $25Hz$.

2.3.2. Modern Implementation
Motional feedback loudspeakers are no longer being produced by Phillips or any other big brands. However, there are researches being done to make digital implementation of motional feedback possible on loudspeakers. In 2013, R. Valk [10] wrote a thesis on enhancing loudspeaker performance at low frequencies by increasing the bandwidth and decreasing THD using motional feedback. The topology used is shown in Figure 2.8, where P represents the loudspeaker and C represents the controller. Firstly, an accurate linear model of the loudspeaker expressed in multiplications of series of transfer functions had been acquired. The controller is then also implemented as a series of transfer functions in order to place zeros and poles at desired locations to compensate for the distortion caused by the loudspeaker. The controller was implemented on a DS1103 PPC Controller Board which was mounted on a PC. The resolution of the used DAC/ADC was 16-bit with sampling frequency of 100kHz. With the controller the THD was reduced by a factor of 11. At a 20Hz high level reference signal, the measured THD was under 4%.

Previously, in one of the groups who also worked in the same project [15], a motional feedback system was designed as seen in 2.7. In this system the analogue power amplifier D provides the loudspeaker
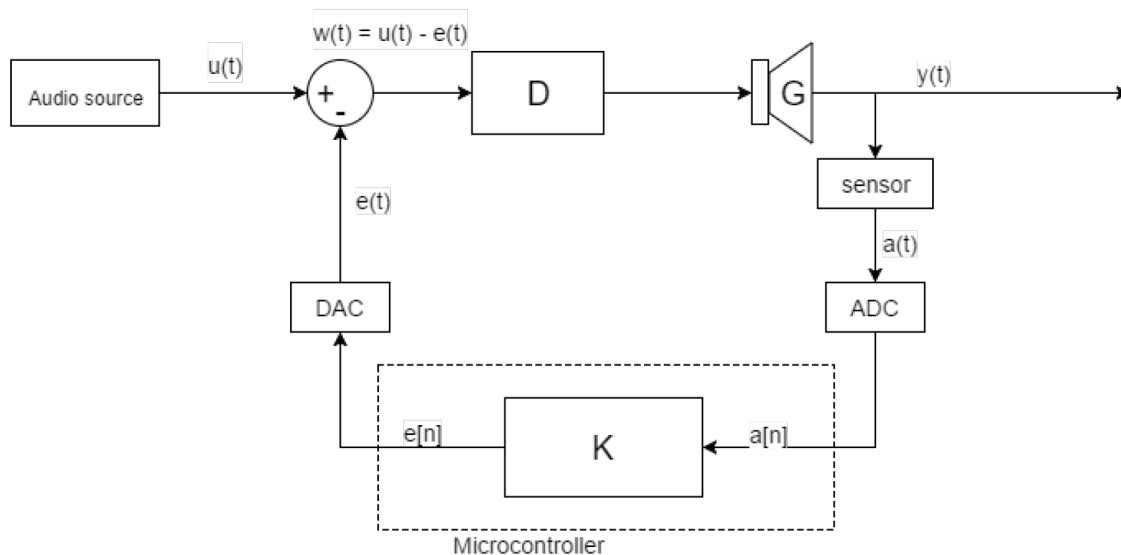

Figure 2.7: Block diagram of the controller. Courtesy of [4].

G with energy while the feedback loop uses a low pass filter implemented with controller K to improve the system. The controller K was meant to be implemented with a micro controller. The controller uses the inverse transfer function to calculate the correction for the input. This inverse transfer function is implemented with a IIR and calculated using system identification. The controller would also contain a low pass filter in order to add zeros in the transfer function to get the same amount of zeros and poles to

enable inversion of the transfer function. From this thesis it is however clear that the introduced delay from a microcontroller is currently still to large to be feasibly used in a feedback loop.

2.3.3. Future work

In the past great THD reduction was achieved, however their bandwidth was still quite small. The purpose of this project is to increase the bandwidth, reduce the THD even more and reduce the costs by means of an analogue implementation.
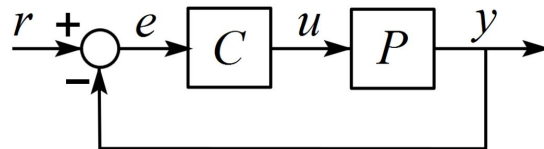

Figure 2.8: Feedback topology used by R. Valk [10].

<div align="right">

3

</div>

Design process

In this section the complete set of steps taken during the design process will be discussed. After understanding the fundamentals of MFB, through the means of a Literature research, and making a feasible plan of action, the design of the analogue controller can be started. In this section every step will be thoroughly explained and justified. The design process is split up in two main parts: the theoretical design process and the practical analogue design process. The first part will mainly discuss the design of a generic controller topology and the second part will cover the mapping of the theoretical design into the analogue domain.

3.1. Theoretical Controller Design

3.1.1. Topology

Choosing a suitable topology for our feedback system will be the foundation upon which the rest of the system will be build on. From the topology is expected that it must reduce the error between the output of the speaker and the reference signal to zero within the specified bandwidth i.e. the output must follow the input signal. In Figure 3.1 a general topology for feedback control, being used, is displayed where $H(s)$ is the plant (including the speaker, sensor and power amplifier transfer), $C(s)$ refers to the controller, $T(s)$ represents the transfer of the sensor used and is assumed to be 1 and $F(s)$ should represent some kind of feed forward controller which is also assumed to be 1. Negative feedback lets the system compare the output of the speaker with the input (reference signal or the desired output) after which the function of $C(s)$ is to correct this error until there is no more error between $y(t)$ and $x(t)$.

$$Y(s) = \frac{C(s) \cdot H(s)}{1 + C(s) \cdot H(s) \cdot T(s)} \cdot F(s) \cdot X(s). \tag{3.1}$$

As mentioned above, the purpose of this topology is to make $Y(s)$ equal to $X(s)$. For this, the scaling factor between $X(s)$ and $Y(s)$ in Equation 3.1 should approximate 1 for all frequencies in the bandwidth. This can be achieved in several ways. Firstly, by using a proportional control for which the gain of $C(s) = K$ is infinite, see Equation 3.2.
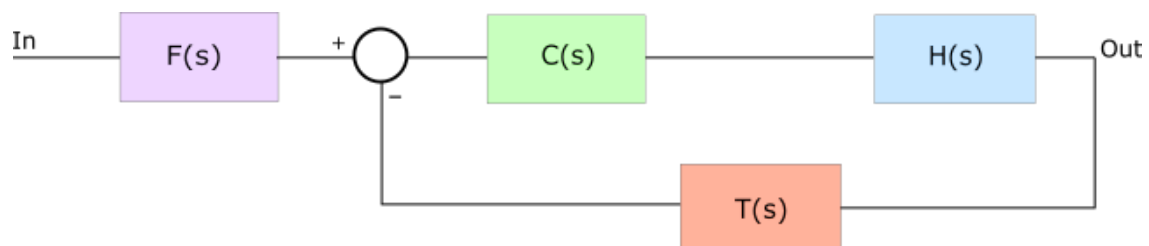

Figure 3.1: General controller topology

$$\lim_{K \to \infty} Y(s) = \lim_{K \to \infty} \frac{K \cdot H(s)}{1 + K \cdot H(s)} \cdot X(s) = X(s). \tag{3.2}$$

Secondly, by designing C(s) in a particular manner in which it corrects the factor depending on the frequency i.e. its amplitude and phase will vary depending on the frequency, effectively keeping the factor 1, which means no high gain is needed. The different ways of implementing this will be discussed in Section 3.1.2.

There are also open-loop control typologies, which only use a feed forward controller (pre-distortion filter). This can easily be implemented for simple linear plants, which is unfortunately not the case for loudspeakers. The possibility exists to combine a feed forward controller with a feedback controller. This will be further discussed in Section 3.1.2.

3.1.2. Controller selection

The selection of the type of controller and how it is implemented eventually determines how the system will work. It is therefore necessary to choose the right controller suitable for this plant. Several controller options where investigated as listed below. In this section these will be compared with each other after which a final controller will be chosen.

The different candidate controllers, which were investigated, are:

1. Feed-forward controller;

2. Proportional-Integrate-Differentiate Controller (PID-controller).

Each controller will be assessed separately in the subsequent sections. The assessment will consist of a brief description of their functioning. Also a list of their advantages and disadvantages will be given, from which a suitable controller implementation will be selected.

3.1.2.1. Feed-Forward Controller

Feed-forward control essentially is designing the inverse of the plant, which will pre-distort the input signal. This will try to cancel out the plant or at least approximately, which can help improve reference tracking or disturbance rejection depending on the topology chosen. The problem however is that feed forward alone is not capable of actively reducing steady-state offset errors [16], which is not the case for feedback controllers. Therefore, a combination of both will significantly improve the total systems performance. For this project the error reduction is of essence. A well known pre-distortion filter is the Linkwitz transform.

3.1.2.2. Linkwitz Transform

Since the estimation of the loudspeaker yields a very high order system, it seems very unlikely that the inverse transfer of the loudspeaker can be build in the analogue domain. Exactly inverting the loudspeaker's behaviour is not possible, but a less accurate approximation can be made using a Linkwitz transform[17][18]. A Linkwitz transform compensates for the response of the loudspeaker at low frequencies. This is demonstrated in Figure 3.2. In this figure the response of the loudspeaker, the Linkwitz transform and the combination is shown. Effectively, it is able to compensate for the resonance peak, as well as the decline in the response for frequencies below the resonance. To create such a Linkwitz transform theoretically, the resonance frequency (F_o) and the quality factor (Q_o) at this frequency of the loudspeaker must be known. Also, the desired frequency (F_p) and quality factor (Q_p) need to be chosen. The transfer function of the Linkwitz transform can then be expressed as follows:

$$LT(s) = \frac{s^2 + 2\pi \frac{f_o}{Q_o} s + (2\pi f_o)^2}{s^2 + 2\pi \frac{f_p}{Q_p} s + (2\pi f_p)^2} \tag{3.3}$$

The transfer function directly follows from the fact that a Linkwitz transform adds a zero at the resonance frequency of the loudspeaker and adds a pole at the frequency to which the response of the loudspeaker stays flat.
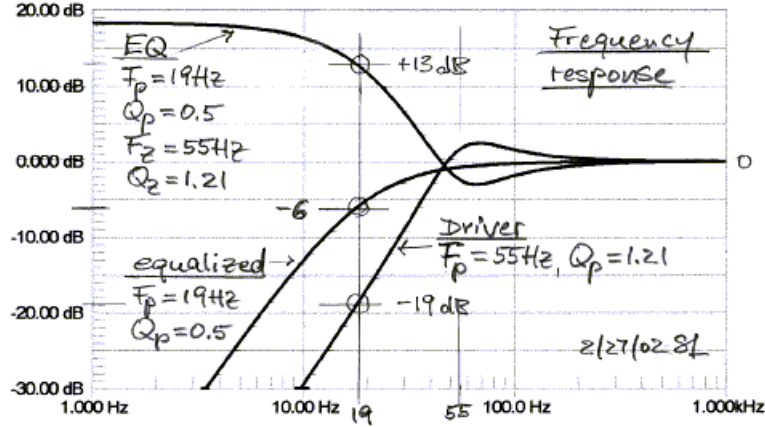
Figure 3.2: The response of the loudspeaker, Linkwitz filter, and the effect of the Linkwitz filter on the response of the loudspeaker. Courtesy of [19].

Theoretically, the Linkwitz transform has a more efficient way to compensate for the linear distortion of the loudspeaker, which means more gain of the controller can be used to compensate for the nonlinear distortion. This will be proven next. The output of the speaker can be written as:

$$V_{out} = \alpha(f)V_{in} + \tilde{v}_o, \tag{3.4}$$

where V_{out} is the output of the accelerometer, V_{in} is the input of the loudspeaker, $\alpha(f)$ is the linear relation between input and output, which is frequency dependent. Essentially this is the linear transfer function of the amplifier, plant and accelerometer combined. $\tilde{v}_o$ is the nonlinear output of the accelerometer. The relation between the input and output including the Linkwitz transform can be written as follows:

$$V_{out} = \frac{\alpha(f) \cdot C \cdot LT}{1 + \alpha(f) \cdot C \cdot LT} \cdot V_{in} + \frac{1}{1 + \alpha(f) \cdot C \cdot LT} \cdot \tilde{v}_o = \beta(f)V_{in} + \gamma(f)\tilde{v}_o. \tag{3.5}$$

Here C is the transfer function of the controller and LT is the transfer function of the Linkwitz transform. The goal of the controller is that the output is equal to the input, which means, according to Equation 3.5, that:

1. $\beta \to 1$,

2. $\gamma \to 0$.

Since a Linkwitz transform compensates for the response of the loudspeaker at low frequencies: $LT \approx \frac{1}{\alpha(f)}$. This means that the objectives reduce to:

1. $\frac{C}{1+C} \to 1$,

2. $\frac{1}{1+C} \to 0$.

Which means that both conditions are achieved by assuring $C \gg 1$. Compared to $\alpha(f) \cdot C \gg 1$ for the system without Linkwitz transform. Since $\alpha(f) < 1$ in general, the controller will have to add much more gain to achieve the same results when not using a Linkwitz transform. Essentially this means when the gain of both controllers in both situations is the same, that the controller can compensate for the nonlinear distortion more when using a Linkwitz transform than not, as the linear response is compensated much more efficiently. This means that the use of a Linkwitz transform is worthwhile when the maximum achievable gain of the controller can not be high enough to meet the requirements. A Linkwitz transform on its own is most effective when its not used in a feedback loop, but it does not suppress the nonlinear distortion. When using it in a feedback system, however, it will not have a high enough performance on its own, as when used in a feedback system, as it does not appear anymore in the two expressions above. Thus when setting $C = 1$, only a quarter of the signal power will be outputted, and half of the nonlinear distortion will remain in the output signal. This means a combination of the controller and Linkwitz transform will be necessary.
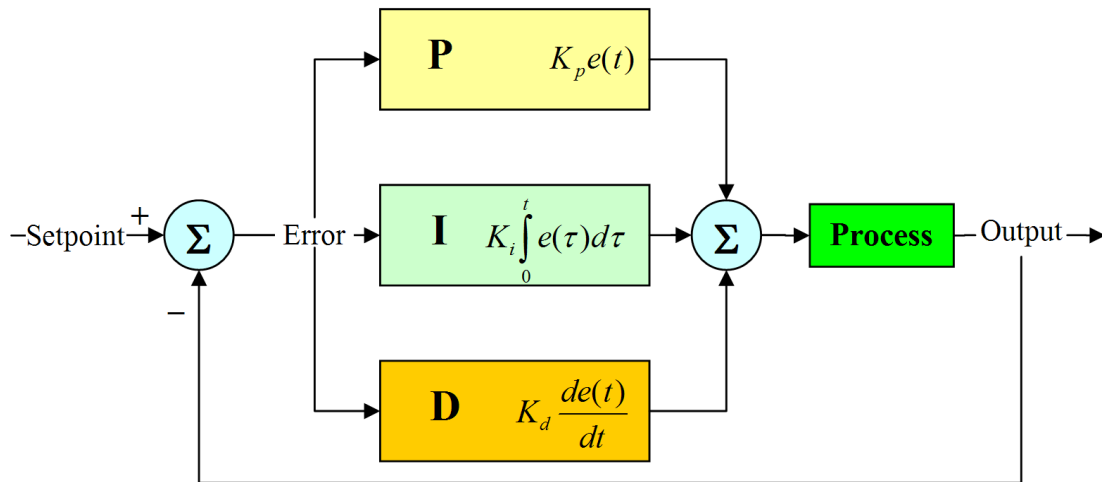
Figure 3.3: PID-controller. Courtesy of [21]

3.1.2.3. PID-Controller

The PID-controller, as the name states, consists of a proportional module, and integration module and a differentiation module. Each of these modules contribute to different behaviours of the controller. The combination of these separate modules is what makes the PID-controller robust and fast [20]. The control function can be expressed as:

$$C(s) = K_p + K_i \cdot \frac{1}{s} + K_d \cdot s. \tag{3.6}$$

This formula can be translated into a circuit, which is illustrated below in Figure 3.3.

Firstly, the P-controller may be enough for correcting minor errors. Generally to reduce the steady state error of more complex plants, the gain of the P-controller needs to be huge. A high gain will indeed cause the error to reduce, but not completely, as well as the reduction of response time. However, it may cause huge overshoots leading to instability [20].

Secondly, the integrator has the capability of reducing the steady-state error and rejecting any disturbance independent of the value of K_i, but the response can be very slow. Increasing the gain will obviously speed up the response, but may introduce instability [20].

Lastly, the differentiator has the capability of improving the stability of the system as well as increasing the speed of the response [20]. Due to its differentiating character the differentiator will counteract radical changes in the transient response, also known as overshoot.

Advantages [22] [20]:

1. Robustness;

2. Fast response;

3. Simple to implement and tune.

Disadvantages[22]:

1. Difficult to handle systems with large delays;

2. May fail to perform as required if the order of the plant is too high.

3.1.2.4. Conclusion

To implement the controller, a PID controller in combination with a Linkwitz transform was chosen. This is because a PID controller is relatively easy to implement and tune, with a robust and fast response. Also the Linkwitz transform was used for more efficient compensation of the linear distortion, such that more gain can be utilised to suppress the nonlinear distortion.

3.1.3. Plant Identification

Before the controller can be designed in detail, the plant that needs to be controlled, in this case the loudspeaker, will have to be identified precisely. The transfer function of the estimated plant is needed to tune the controller correctly. Because of the fact that a PID controller works optimally for linear systems, a linear estimation of the system will be done. Firstly, the frequency response of the plant, which includes the amplifier, loudspeaker and accelerometer, was measured. The measurement setup is illustrated in Figure 3.4. A signal is generated in the sound card connected to a computer and is then passed to a connection box, which was provided to us. The output of this box is passed into the system which includes the amplifier, speaker and finally the accelerometer. The output of the accelerometer is again passed through the connection box which passes it to the sound card again. The capacitor at the output of the accelerometer is used to remove the offset in the output signal of the accelerometer. Then using a Matlab script, the frequency response can be calculated. This Matlab code is the same as the code that is written for the first year project 'EPO 1: Booming Bass' of the Bachelor Electrical Engineering program at TUDelft [23]. The Matlab code works by sending a pseudo-noise signals with a nearly flat frequency spectrum into the sound card. This goes through the system, and the sound card then records the output of the accelerometer. Then the frequency response is calculated by dividing the output by the input in the frequency domain. The frequency response includes the response of the amplifier, loudspeaker and accelerometer. The obtained frequency response can be seen in Figure 3.5.
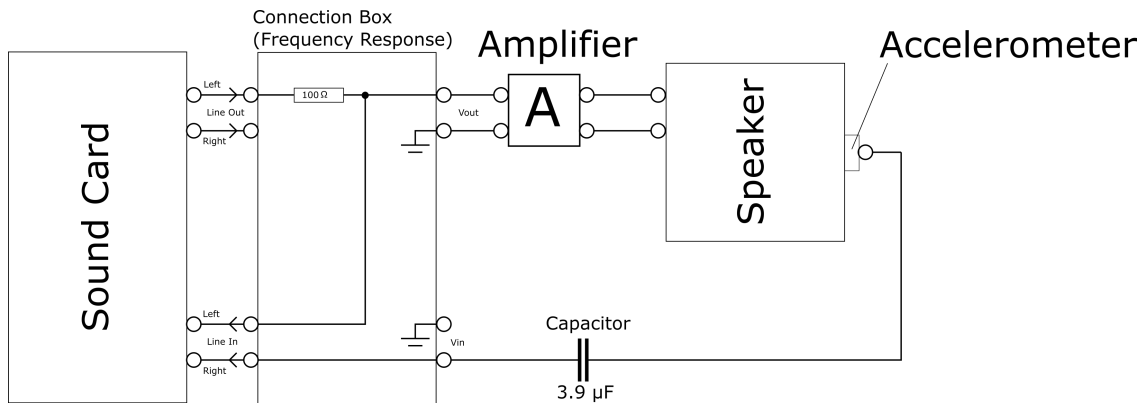

Figure 3.4: The measurement setup for measuring the frequency response of the Amplifier-Loudspeaker-Accelerometer system. Notable is the capacitor at the output of the accelerometer, which is used to remove the offset of the accelerometer.

Subsequently, using another Matlab script the transfer function of the plant can be estimated. The central part of this script is the function *'tfest'*, which is part of the Matlab *System Identification Toolbox*. The algorithm used in this estimation essentially solves a nonlinear least-squares problem. The exact details of this algorithm are discussed in [24]. The response was limited to the range $10Hz \leq f \leq 400Hz$, because it was essential that the transfer function would fit this part of the response with high accuracy, since the main MFB operation is within this range. The resulting transfer function had a 96% fit to the frequency response and was of order 9. In Figure 3.5 the bode plots of both the measured frequency response of the plant as well as the estimated transfer function can be seen. At $20Hz$, the output of the system is $-23dB$. Because of the fact that the estimated transfer function only considered the plant response in the range $10Hz \leq f \leq 400Hz$, the transfer function might not be an accurate representation of the plant outside this range. This will have to be taken into account when designing the different parts of the system, as well as not relying on results of simulations with frequencies outside this range.

Before moving on, the stability of the acquired transfer function will need to be investigated. To check this, a Nyquist plot and a root locus plot can be used. These can be seen in Figure 3.6 and Figure 3.7. From the root locus plot, it can be seen that no poles are present with real parts of more than 0, which means that the system is stable. It can be seen that no poles will ever move to the right of the imaginary axis when increasing the gain, thus the system will remain stable in closed loop, even when increasing the gain. Finally, from the Nyquist plot it can be seen that the plot does not encircle the point -1, which again confirms stability. Finally, the gain margin and phase margin of the plant can be calculated using Matlab,

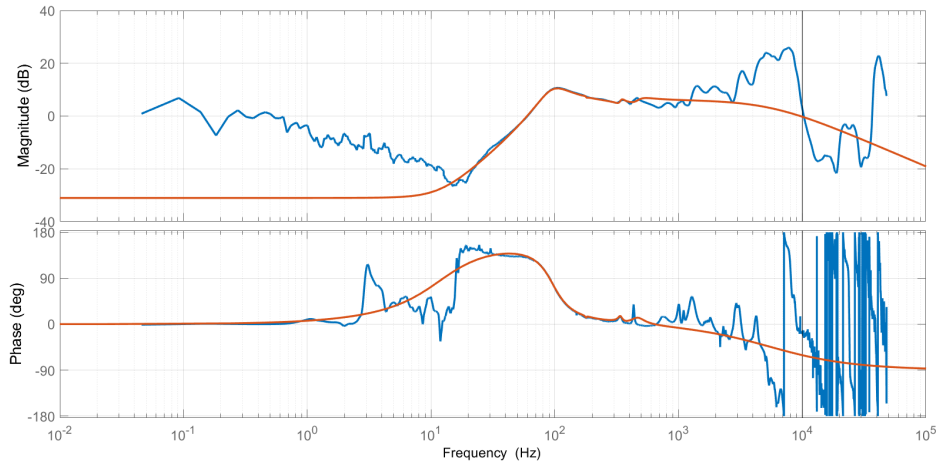of which the results can be seen in Figure 3.8.

Figure 3.5: A Bode plot of both the measured frequency response of the plant as well as the estimated transfer function of the plant.
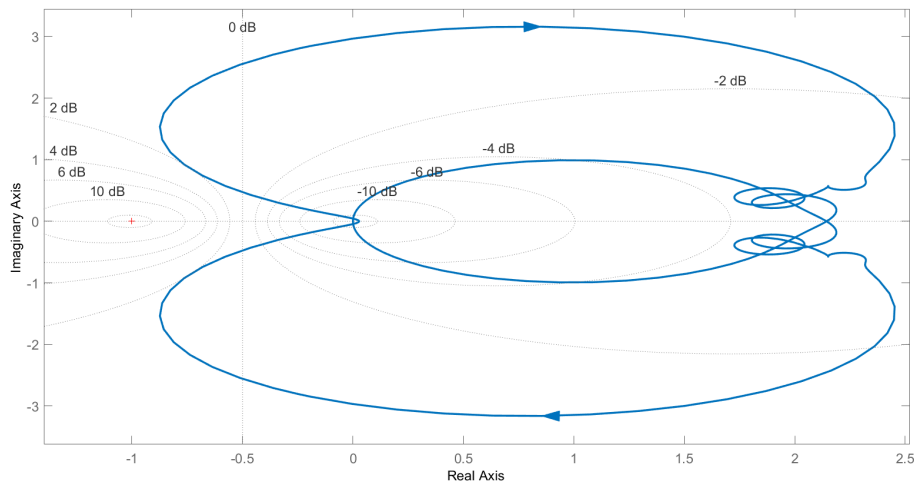

Figure 3.6: A Nyquist plot of the estimated plant. From this can be seen that the system is stable, as the plot does not encircle the point -1 once.

3.1.4. PID tuning

The next step is to design the PID-controller specifically for the estimated plant. The PID-controller is required to be robust and have a fast enough response time. By tuning the parameters of the PID, its behaviour can be adjusted until a fast response and robust behaviour is reached. There are several methods of tuning. The most commonly known manual tuning methods, also the ones which were treated in the same course previously mentioned, are the two Ziegler-Nichols methods, namely the Ultimate Gain method and the Quarter decay ratio method. Matlab has PID-controller tuning capabilities within the Simulink operations, which are automatic. Below these methods will be discussed separately. Also the advantages and disadvantages will be listed [20].

For the Ultimate Gain method the ultimate gain (K_u) has to be determined and its corresponding oscillation
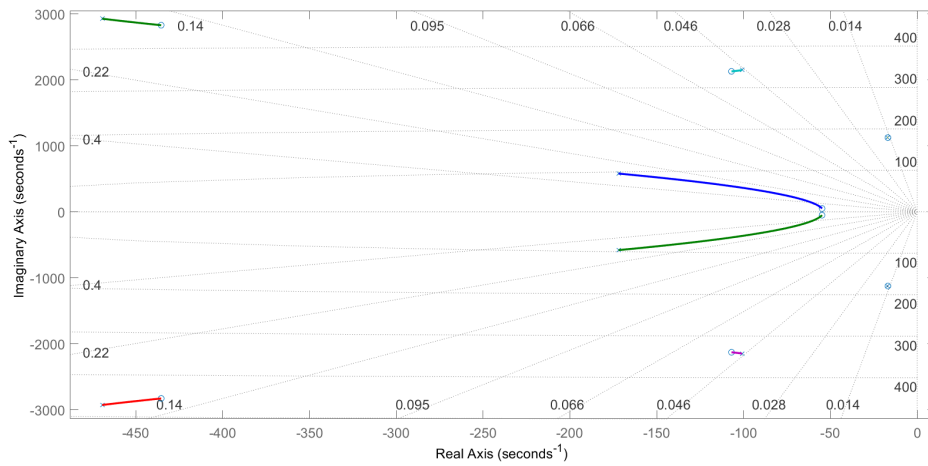
Figure 3.7: A Root Locus plot of the estimated plant. In this can be seen that no poles are present in the right hand side of the imaginary axis, and will never move there when increasing the loop gain, which means the system is stable. A pole at position $-3.492 \cdot 10^4$ which moves towards $-\infty$ as the loop gain increases, is also present in the Root Locus, but is not depicted for clarity.
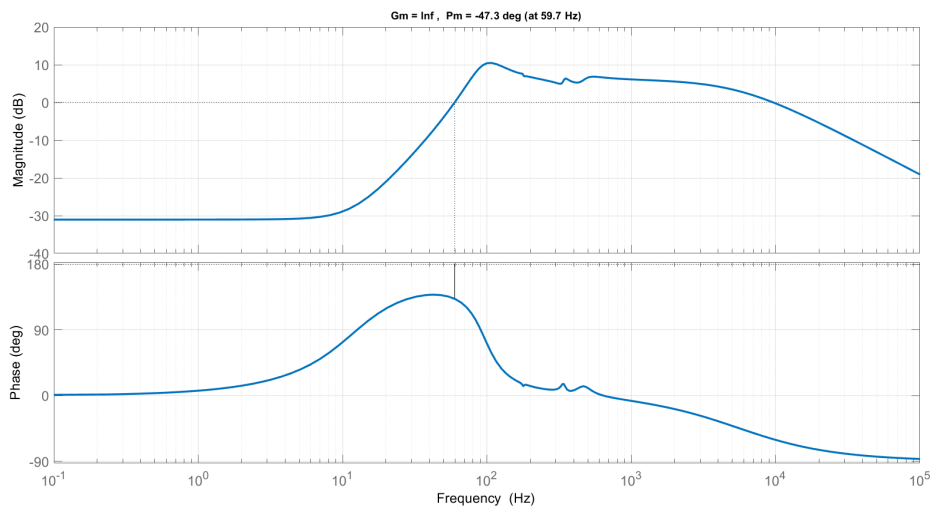

Figure 3.8: Again the Bode plot of the estimated transfer function, but this time the gain margin (Gm = ∞) and phase margin (Pm = -47.3ř) are also indicated
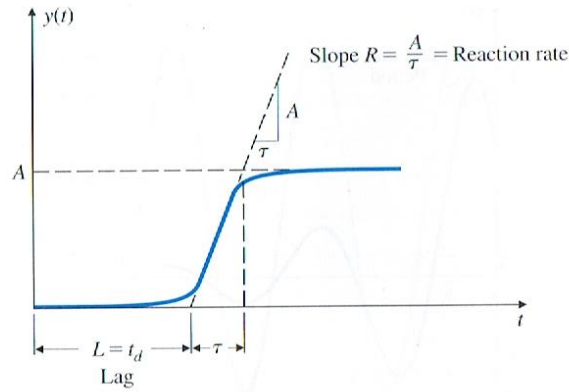
Figure 3.9: S-shape process curve. Courtesy of [20]

period (P_u). The ultimate gain is obtained by increasing the K of Equation 3.1.4 until the system becomes marginally stable. A system is marginally stable when the the output keeps oscillating i.e. one pole is located on the imaginary axis causing oscillation. After establishing K_u, the period of the oscillating output can be determined by observation. Using the obtained parameters and the equations below, T_i and T_D can be calculated for the PID-controller.

$$C(s) = K \cdot (1 + \frac{1}{T_i \cdot s}) + T_D \cdot s. \tag{3.7}$$

For the P-controller:

$$K = 0.5 \cdot K_u. \tag{3.8}$$

For the PI-controller:

$$K = 0.45 \cdot K_u$$
$$T_i = \frac{1}{1.2} \cdot P_u \tag{3.9}$$

For the PID-controller:

$$K = 0.6 \cdot K_u$$
$$T_i = 0.5 \cdot P_u$$
$$T_D = \frac{1}{8} \cdot P_u \tag{3.10}$$

The quarter-decay method uses the assumption that for many systems the step response can be approximated by an S-shape process curve as illustrated in Figure 3.9 with the transfer function :

$$\frac{Y(s)}{U(s)} = \frac{A \cdot e^{-s \cdot t_d}}{\tau \cdot s + 1} \tag{3.11}$$

The idea is that parameters are tuned in such a way that the closed-loop transient step response results in a decay of about 0.25 i.e the oscillation/overshoot decays with a factor of approximately 0.25 within one period. From simulations done in the past the following formulas further describe its application:

$$D_c(s) = K_p(1 + \frac{1}{T_I \cdot s} + T_d \cdot s) \tag{3.12}$$

For the P-controller,

$$K_p = \frac{1}{R \cdot L}. \tag{3.13}$$

For the PI-controller:

$$K_p = \frac{0.9}{R \cdot L}$$
$$T_i = \frac{L}{0.3}. \tag{3.14}$$

Lastly, for the PID-controller:

$$K_p = \frac{1.2}{R \cdot L}$$
$$T_i = 2L \tag{3.15}$$
$$T_s = 0.5L.$$

The last method is the least labour intensive, the least time consuming and most accurate way of tuning the PID-controller parameters suitable for the plant, namely the automatic PID-tuner located in Simulink. These parameters can be tuned to the desired robustness and response time. The parameters can also be changed manually. The system also illustrates the result of the tuned parameters versus the untuned parameters. The results of this method and it verification will be further discussed in Section 3.1.6.

3.1.4.1. Final Choice

The Ziegler-Nichols tuning methods are mainly meant to roughly estimate parameters of the PID-controller. Both of these methods have been tested, but resulted in poor performance results. After calculating the parameters these need to be verified by means of simulations. The problem with these methods is that every trail needs to be calculated manually and requires eye-balling to obtain for example the ultimate gain. Eventually time was lost trying to tune the controlling with poor results. After stumbling upon the tuning add-on in Simulink less effort had to be put in obtaining accurate results, of course this is only an application in Simulink and needs verification. In Section 3.1.6, the feasibility of the obtained parameters have been tested in terms of stability and distortion rejection.

At the end, the automatic tuning-add on in Simulink was used to tune the PID-controller fit to meet the requirements.

3.1.5. Tuning Result

In Section 3.1.3 the frequency response of the system was estimated. Using this data, the PID-controller was tuned in Simulink using the application, which resulted in a PI-controller. The value of the differentiator part was negligible. The PI-controller equation is given below in Equation 3.16. The tuning result had to comply to two requirements. Firstly, the step response of the complete system has to have a maximum deviation of 0.1% to meet the THD reduction requirement. Secondly, the controller has to have a maximum response time of $\tau = \frac{1}{2f_{max}} = 1.67ms$, to ensure the controller's response is fast enough for $f_{max} = 300Hz$. However, since this is very critical for correct functioning, the maximum response time was lowered to $\tau = 0.5ms$, to support even $1kHz$ signals. The results of the parameters are $K_p = 1$ and $K_i = 35000$, note that K_i is quite large.

$$C(s) = K_p + \frac{K_i}{s}. \tag{3.16}$$

Before continuing with the design it was tested mathematically whether the PI-controller could deliver reasonable simulation results. The fact that the speaker will show non-linear behaviour at the output in the form of harmonics needs to be taken into account. The output can again be expressed as a sum of a linear transformation from input V_{in}, to output, V_{out}, and a general nonlinear distortion term $\tilde{v}_o$, see Equation 3.17.

$$V_{out} = \alpha(s)V_{in} + \tilde{v}_o, \tag{3.17}$$

where $\alpha(s)$ is some linear function. The output can be expressed as:

$$Y(s) = \frac{(K_p + \frac{K_i}{s}) \cdot P(s)}{1 + (K_p + \frac{K_i}{s}) \cdot P(s)} \cdot V_{in}(s) + \frac{1}{1 + (K_p + \frac{K_i}{s}) \cdot P(s)} \cdot \tilde{v}_o. \tag{3.18}$$

$$\lim_{s \to 0} Y(s) = \lim_{s \to 0} \frac{(K_p + \frac{K_i}{s}) \cdot P(s)}{1 + (K_p + \frac{K_i}{s}) \cdot P(s)} \cdot V_{in}(s) + \frac{1}{1 + (K_p + \frac{K_i}{s}) \cdot P(s)} \cdot \tilde{v}_o = V_{in}(s). \tag{3.19}$$

Then the steady state result is obtained by taking the limit of $s \to 0$, which corresponds to steady-state in the time domain, as can be seen in Equation 3.19. This clearly illustrates that the distortion component is rejected successfully and the output will follow the reference signal. The question now is how long will it take for the PI-controller to obtain this result. Because of the high integrator value, the value of s does not need be that small for the value will remain dominantly high compared to the other parameters. The fraction may still be approximated as unity. This is also fortunate due to the fact that low values for $s = j\omega$ corresponds to low frequencies, meaning that the PI-controller corrects more intensively at lower frequencies as required. For higher frequencies the plant does not introduce large linear and non-linear distortion, thus not much gain is needed. The PI-controller can be seen a frequency dependent gain regulator i.e. the gain of the controller increases at frequencies where it is most needed to ensure proper error correction and fast response time. Of course this is a rough verification and will be further justified in Section 3.1.6, where the accuracy of it will be investigated in more detail. Also the stability and robustness of the system will be investigated in more detail.

3.1.6. Matlab and Simulink Simulations

The resulting PID controllerhas been simulated in Matlab and Simulink to check the effectiveness and stability. First the PID controller was tested in Simulink for different input frequencies: $20Hz$, $50Hz$ and $100Hz$. The Simulink schematic can be seen in Figure 3.10 and the results can be seen in Figure 3.12, 3.13 and 3.14. For comparison, the response of only the plant for frequencies in the range of $10Hz \le f \le 300Hz$ can be seen in Figure 3.11. From comparing the three responses to the original response, it can be seen that the response of the system has been improved greatly, and that the output of the accelerometer follows the input signal nicely. However, these plots only give a qualitative simulation of the effect of the controller. Thus to efficiently check for all frequencies, the Bode plot of the total controlled system is shown in Figure 3.15, and a magnified version is shown in Figure 3.16. From this it can be seen that the response of the system is almost flat in the range of $10Hz \le f \le 300Hz$, with a minimum magnitude of $-0.301dB$ at $20Hz$. The controlled system seemingly also behaves nicely outside this range, even up to frequencies of $10kHz$, however, the plant estimation is inaccurate above frequencies of $400Hz$. This also means that the results of the controlled system are also inaccurate above $400Hz$. Compared to the original magnitude of $-23dB$, this is an increase in power of $20.699dB$ or 117.44 times. This large gain comes at a price, however, as the output voltage of the PID controller is much higher than the allowed $V_{out;max} = 0.75V$. This maximum allowed output voltage of the PID controller comes from the fact that only $V_s = [-20V, 20V]$ is available, and that the amplifier has an amplification of $A_v = 20 \approx 26dB$. This means that the maximum allowed output of the PID controller is $V_{out;max} = \frac{|V_{s;max}|}{A_v} = \frac{20}{20} = 1V$, which is lowered slightly to $V_{out;max} = 0.75V$ for safety, because if this maximum voltage is exceeded, the amplifier will start to clip, causing the loudspeaker output to be highly distorted. This maximum output voltage will mainly be exceeded at low frequencies, as amplifications of as high as 10 times are needed. This means
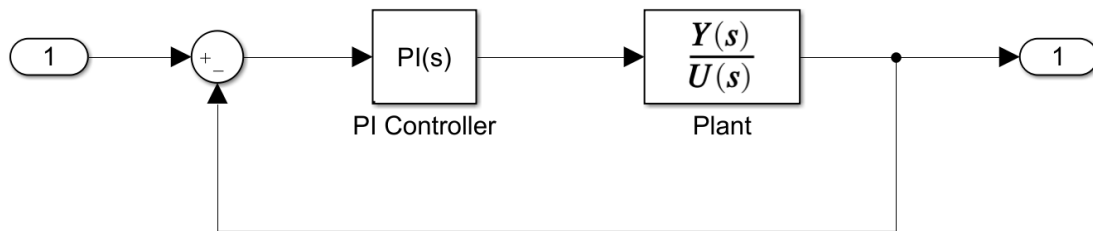
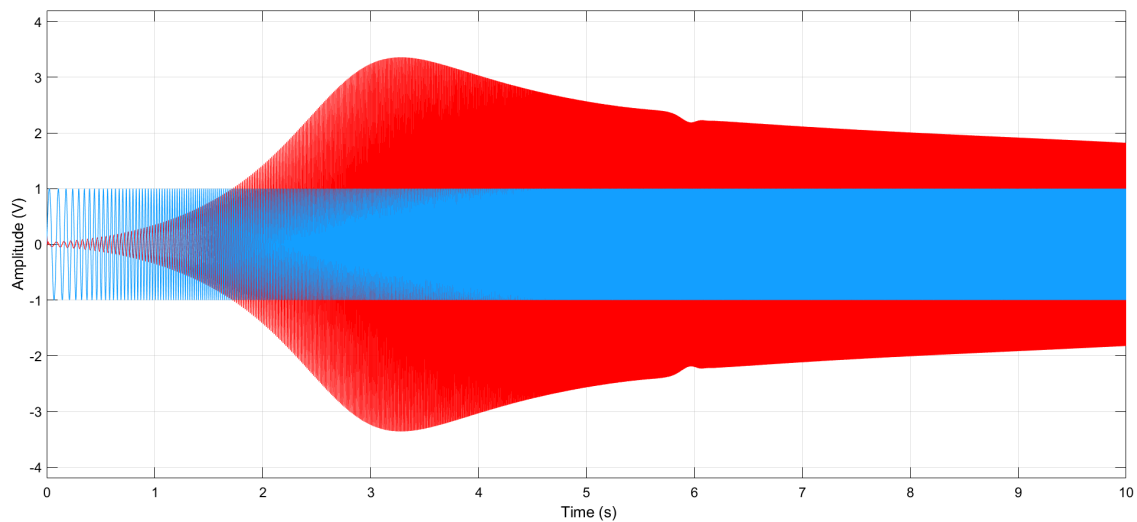Figure 3.10: The schematic of the PI controller and plant system in Simulink.

Figure 3.11: The output of the plant (in red) when a frequency sweep of $10Hz$ to $300Hz$ (in blue) is applied.

that the input voltage V_{in} of the system should be lowered to a value such that $V_{out} \leq V_{out;max}$. This value for the input voltage can be calculated for all frequencies, which can be seen in Figure 3.17.

Subsequently, the stability of the controlled system will have to be checked. This can be done using a Nyquist plot and a pole-zero plot. These can be seen in Figure 3.18 and 3.19. From the Nyquist plot it can be seen that the system is stable, as the plot does not encircle the point -1. In the pole-zero plot, it can also be seen that the system does not have any poles to the right of the imaginary axis, which also confirms the system is stable.

Now that the effectiveness and stability of the controller have been theoretically confirmed using simulations, the analogue controller and other circuits, which are needed for correct functioning, can be designed. The design process of the analogue implementation of the controller can be seen in Section 3.2.
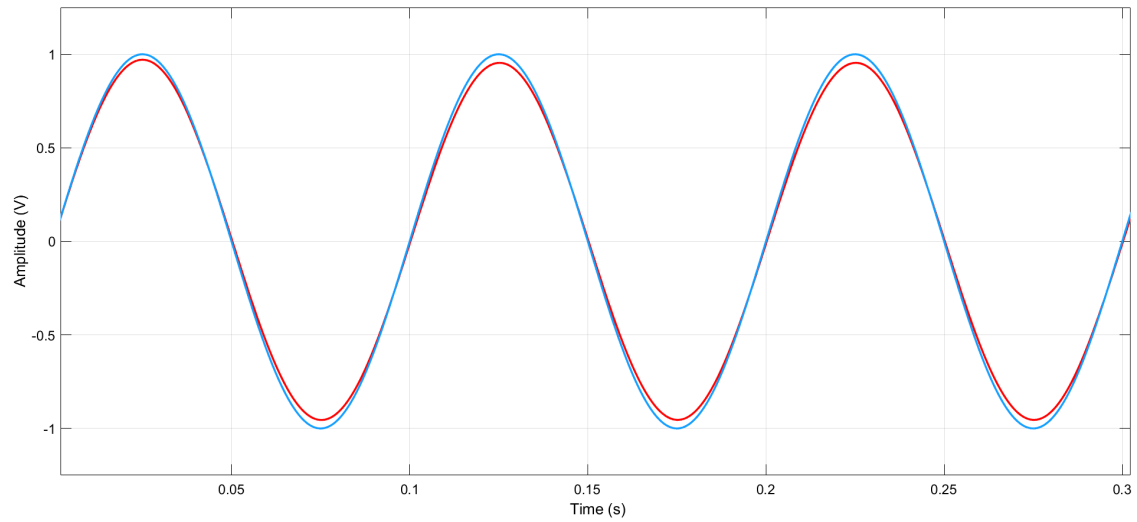
Figure 3.12: The output of the system (in red) when a sine signal of $20Hz$ is applied (in blue)
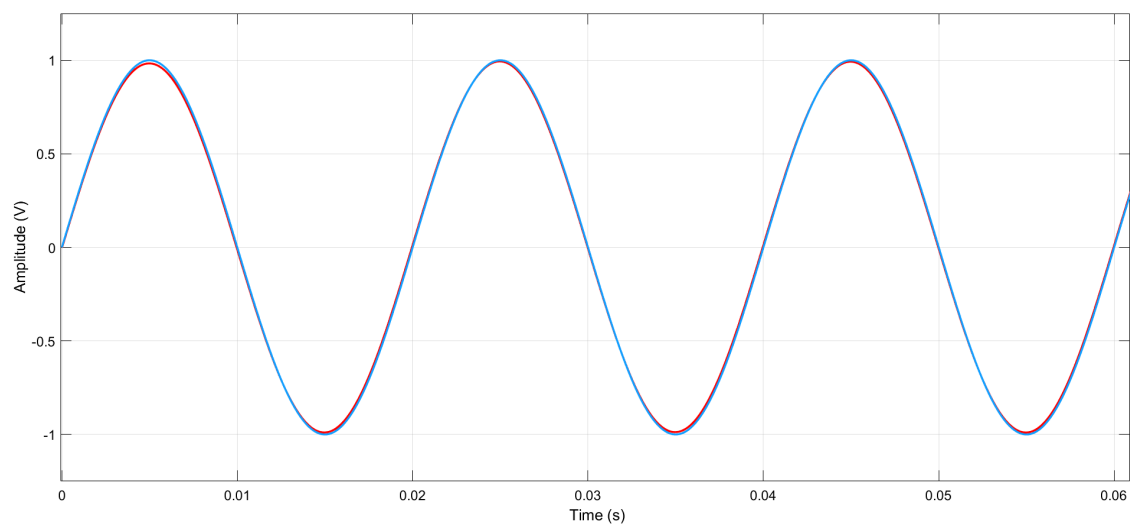

Figure 3.13: The output of the system (in red) when a sine signal of $50Hz$ is applied (in blue)
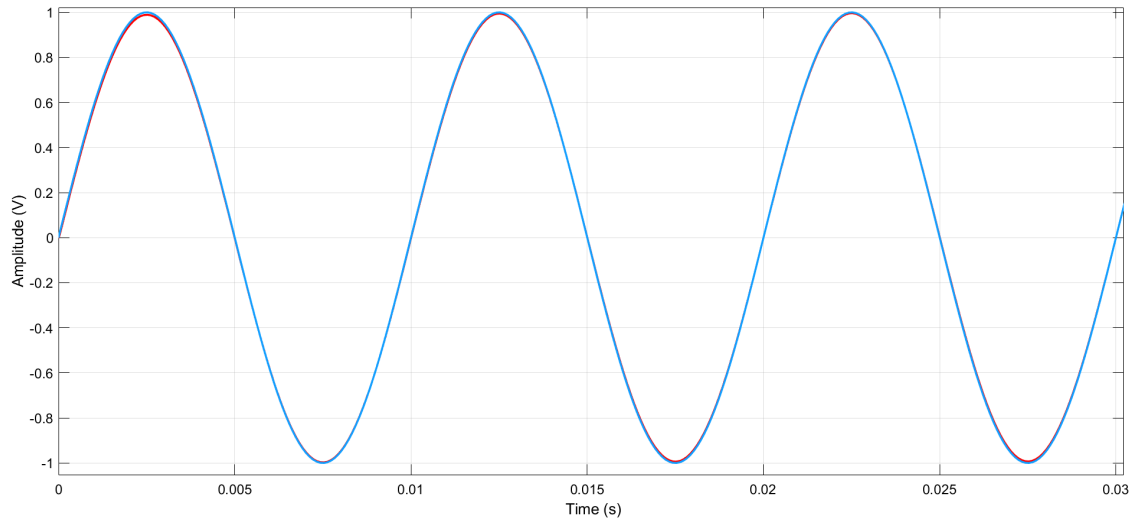
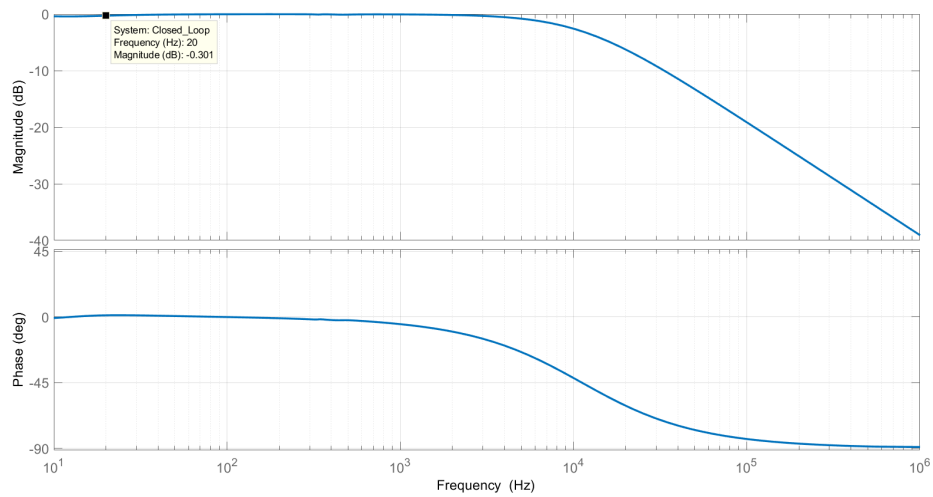Figure 3.14: The output of the system (in red) when a sine signal of $100Hz$ is applied (in blue)

Figure 3.15: Bode plot of the controlled system. It can be seen that the response is relatively flat, with a minimum value of $-0.302dB$.
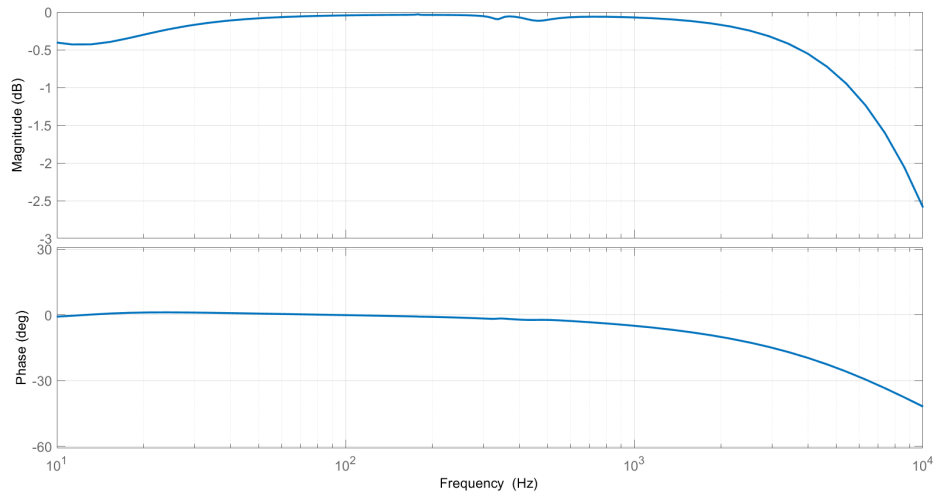
Figure 3.16: Bode plot of the controlled system, closed up, such that the deviations from $0dB$ are much more visible.
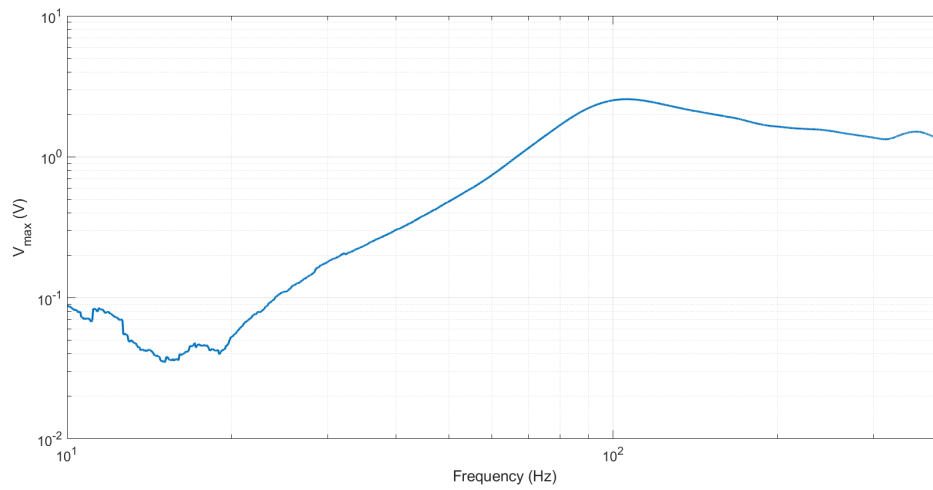
Figure 3.17: The maximum input voltage of the system dependent on the frequency.
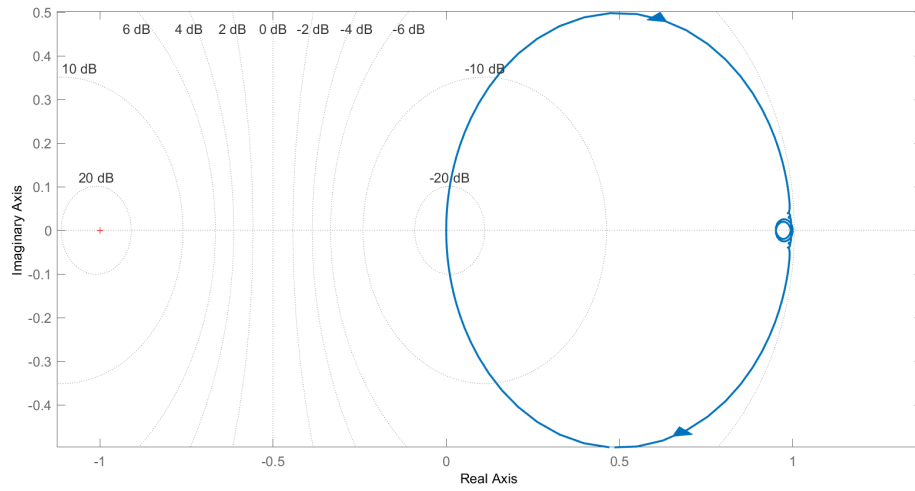
Figure 3.18: The Nyquist plot of the controlled system. It can be seen that the plot does not encircle the point -1, which means the system is stable.
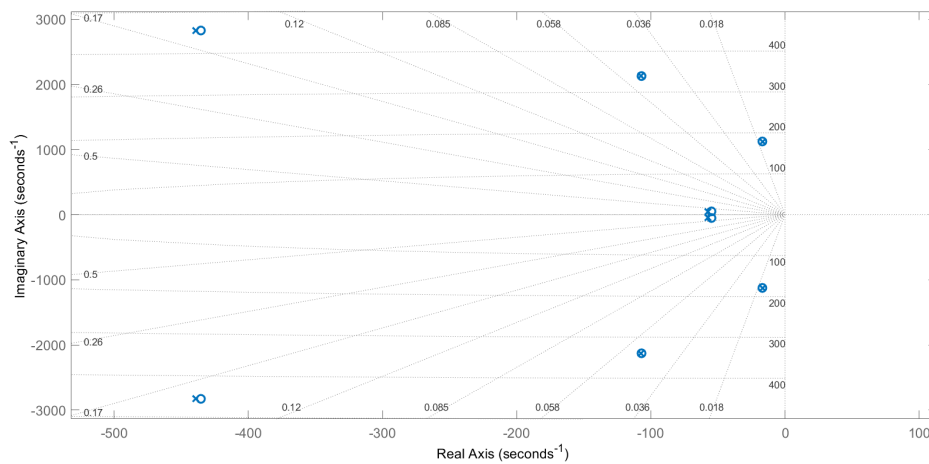
Figure 3.19: The pole-zero plot of the controlled system. Notable is that there are no pole to the right of the imaginary axis, which confirms stability of the system. This plot is zoomed in, to increase visibility. There are two poles (at $-7 \cdot 10^4$ and $-3.51 \cdot 10^4$) and one zero (at -3.5e4), which is not visible in this plot.

3.2. Analogue Implementation

First the analogue design and implementation of the PI controller will be discussed, as this is the core of the control system. Subsequently, peripheral circuits, which are needed for correct functioning of the system, are discussed. Finally, the design of some additional filters are discussed. These filters are needed to disable the MFB at high frequencies, since the feedback signal is not reliable anymore, and the controller will not function correctly anymore.

3.2.1. Analogue PI controller

The PI controller consists of a proportional and an integrating term. These can essentially be designed individually, and subsequently be added together. The proportional term can be implemented using a simple amplifier, and the integration term can be implemented using an integrator. As will be seen, the P and I terms will not have to be designed individually, but a single circuit can be used to implement both.

3.2.1.1. Integrator

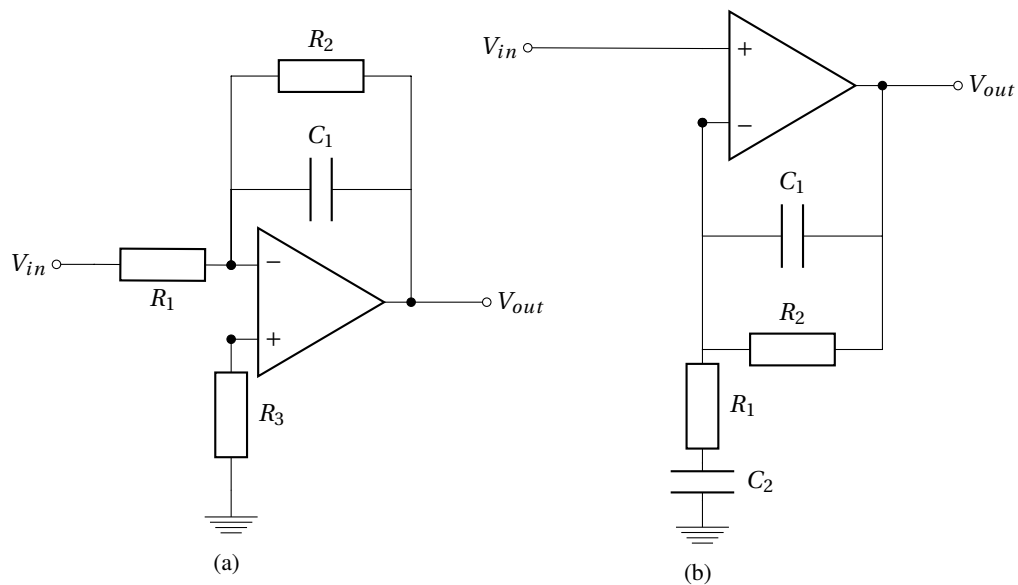There are two possible integrator topologies:

(a)

(b)

Figure 3.20: Two different implementations of an integrator. In (a), a simple integrator is depicted. In (b), a voltage amplifier with a capacitor in parallel to the second resistor, to create the integrating behaviour, is depicted.

The first, which can be seen in Figure 3.20a, is a simple implementation of an integrator. Two additional resistors have been added to prevent undesirable behaviour of the integrator. Firstly, resistor R_2 is used to make sure that the DC-loop gain is finite. Secondly, resistor R_3 is used to compensate for the bias current of the op amp. The transfer function of the integrator can be written as follows, neglecting the offset voltage and bias current for simplicity:

$$H(s) = -\frac{R_2}{R_1} \cdot \frac{1}{1 + sR_2C} \approx \frac{K_i}{s} \tag{3.20}$$

This means that for $f >> \frac{1}{2\pi R_2 C}$, $K_i = \frac{1}{R_1 C}$. For this circuit also an additional inverter is needed, as the input signal is inverted on top of being integrated. The offset voltage will be amplified by a factor $-\frac{R_2}{R_1}$, which will means this circuit is not suitable. This is because the integrator constant is high, which means clipping is an issue that could arise when a large offset is induced in the integrator.

The second implementation can be seen in Figure 3.20b. This is essentially a voltage amplifier with two additional capacitors. The first capacitor, placed in parallel with resistor R_2, is used to create an integration behaviour, for which the integrator constant, K_i, is also calculated by $K_i = \frac{1}{R_1 C_1}$. The second capacitor

is used to prevent the DC offset voltage from being amplified by the same amount as the input signal. Essentially, R_1 and C_2 form a high pass filter which causes the offset voltage not to be amplified. When the frequency is higher than the cutoff frequency of this filter and higher than the cutoff frequency of the filter caused by C_1 and R_2, and when neglecting the offset voltage and bias current, the transfer function of this integrator implementation can be written as follows:

$$H(s) = 1 + \frac{1}{sR_1C_1}.$$ (3.21)

This circuit has three advantages:

1. The output of the integrator is non-inverting, meaning no additional inverter is needed.

2. The transfer function of the integrator shows an additional term, which corresponds to the proportional term of the PI controller, of which the proportional constant $K_p = 1$. This is very convenient, as this value is very close to the optimal value. Also, this means no adder is needed two combine both P and I terms.

3. This implementation is able to remove a lot of the offset that will be created with a high integrator constant.

However, the offset of the integrator still is not completely removed. This is because bias currents will still flow through the resistor R_2, creating voltages at the output of $R_2 \cdot I_b$, with I_b being the bias current of the negative input port of the op-amp. Some time was lost to resolve this problem, however, a third implementation, which is seen in Figure 3.22, solves this problem. In this figure, the bias current and offset voltage sources are also indicated. Three input sources are present: The normal system input, V_{in}, the accelerometer output V_a and an offset source of $2V$. These were included to test for offset removal. In the actual circuit, these would not be present. Firstly, the integrator gain is split into two parts: The first part is a regular voltage amplifier with a gain of 25, also equipped with a capacitor to remove the amplification of the offset voltage. And the second part is the second integrator discussed above. Splitting the integrator gain in this way partly solves the problem of having too large of a gain in a single amplifier, decreasing the gain in bias current and offset voltage. Also, a high-pass filter is added at the end to remove the offset that is still present in the signal. Since audio signals are not uni-polar, polar capacitors cannot be used. Thus, an additional offset is added to the input signal. This way, polar capacitors can be used, as one side of the capacitor will always stay at a higher voltage than the other side. This offset is also filtered out by the high-pass filter at the end. Alternatively, audio capacitors can be used, which means the additional offset is not needed as well. Additionally, a low-pass filter is also present at the end of the circuit. This filter is optional, and will be described in more detail in Section 3.2.4.2. The only disadvantage might be the fact that now the proportional term shifts from $K_p = 1$ to $K_p = 25$, which could have devastating effects. In Figure 3.21 the bode plot of this changed controller can be seen. Notable is that there is a drop of $-1.4dB$ at $11Hz$, also, after $200Hz$, there is an error present of $-0.17dB$. This means that now the controller does not function as correctly anymore. However, this will be partly fixed when combined with a Linkwitz transform as will be seen in Section 3.2.2. The simulations of both the second and third implementation can be seen in Figures 3.23. Here can be seen that the second implementation still has offset in the output signal, while the third implementation does not. Also, the frequency response of both implementation is the same, which confirms the third implementation will function correctly.

3.2.2. Linkwitz Transform

The Linkwitz transform is a mathematical transformation that basically tries to compensate for the linear distortion of the speaker. It is essentially meant as a pre-distorting filter that approximates the inverse transfer of the speaker. The mathematical description and workings of the Linkwitz transform are described in Section 3.1.2.2. The analogue implementation of the Linkwitz transform can be seen in Figure 3.24. Before calculating the values for the resistors and capacitors, however, the feasibility of the chosen Q_p and f_p, will have to be checked. This can be done using Equation 3.22 [18]:

$$k = \frac{\frac{f_o}{f_p} - \frac{Q_o}{Q_p}}{\frac{Q_o}{Q_p} - \frac{f_p}{f_o}},$$ (3.22)
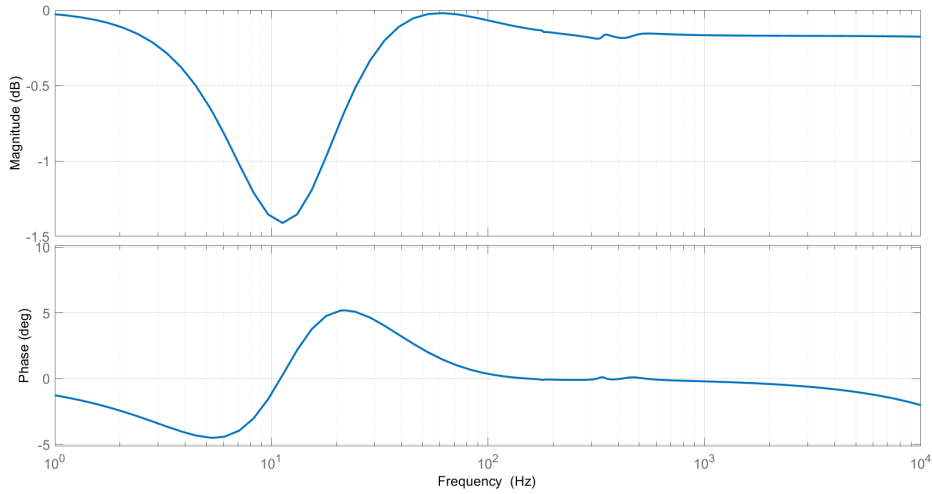
Figure 3.21: The Bode plot of the system response for controller values of $K_p = 25$ and $K_i = 10000$.
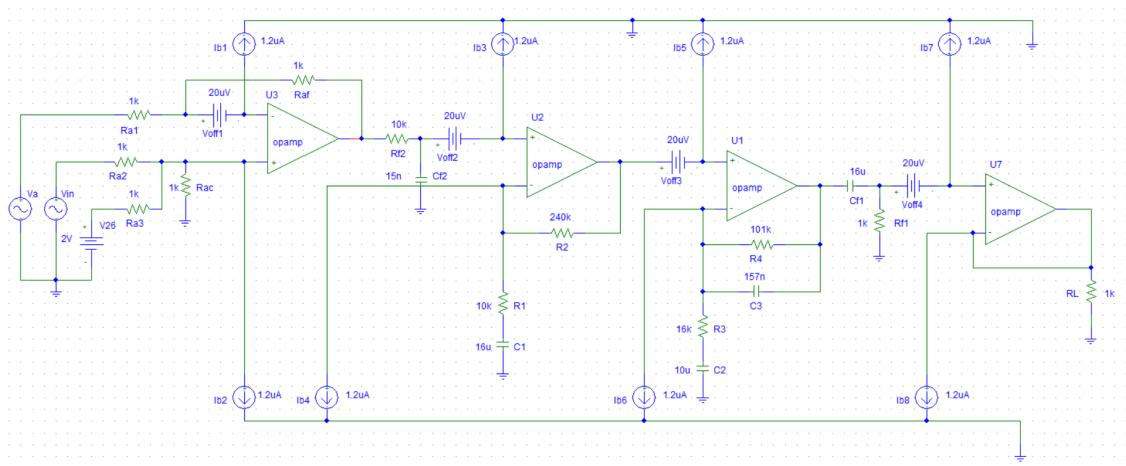
Figure 3.22: The schematic of the PI controller. V_{in} represents the input signal, V_a represents the output of the accelerometer. A load is connected to the output of the controller for the sake of simulation. Notable is the addition of a low-pass filter in front of the integration part of the controller. For the purpose of this filter see Section 3.2.4.2. Additionally, bias current and offset voltage sources are added to each op amp, and only serve for simulation purposes, and thus will not be present in the actual circuit.
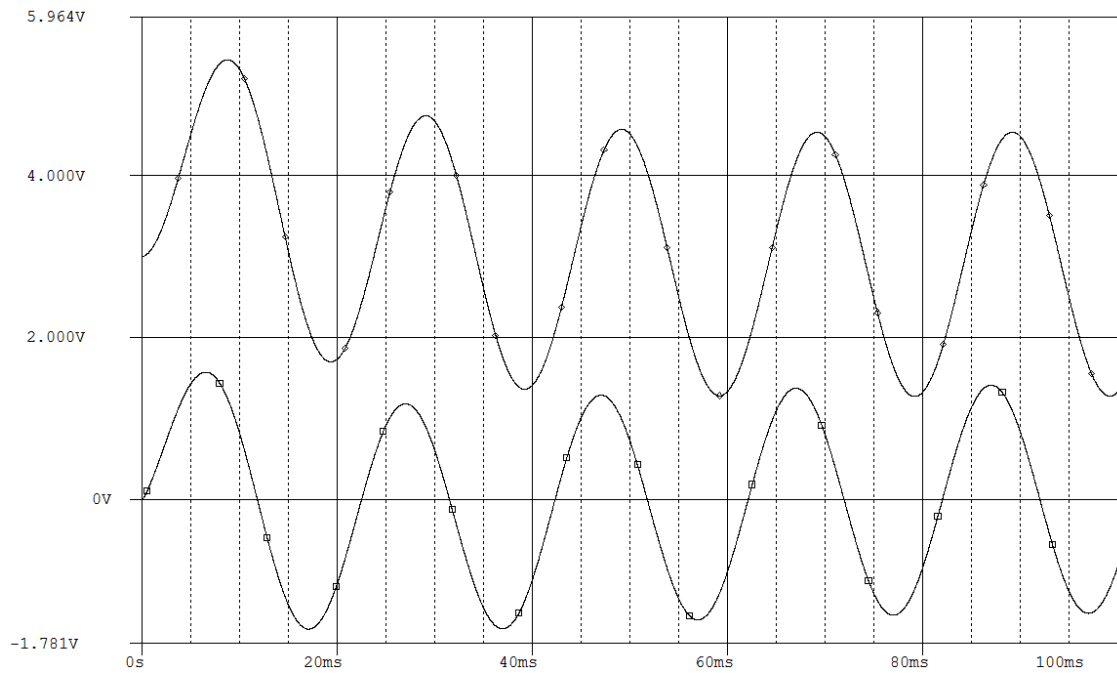
Figure 3.23: The simulation of implementation 2 (upper graph) and implementation 3 (lower graph) for an input signal of $50Hz$ and amplitude of $50mV$. It can be clearly seen that implementation 2 still has an offset present in its output, while implementation 3 has a negligible offset.

Figure 3.24: The schematic of the Linkwitz transform. Courtesy of [18].

for which $k > 0$ is required. For values of $f_o = 91Hz$, $Q_o = 2.2$, $f_p = 10Hz$ and $Q_p = \frac{1}{\sqrt{2}}$, $k = 1.9949$. A plot of the theoretical Linkwitz transform is also displayed in Figure 3.25. This can later be used to compare to the analogue version of the transform. Then, using Equations 3.23 to 3.28[18], the component values can be calculated.

$$Choose\ C_2, \tag{3.23}$$

$$R_1 = \frac{1}{2\pi f_0 C_2 [2Q_o(1+k)]}, \tag{3.24}$$
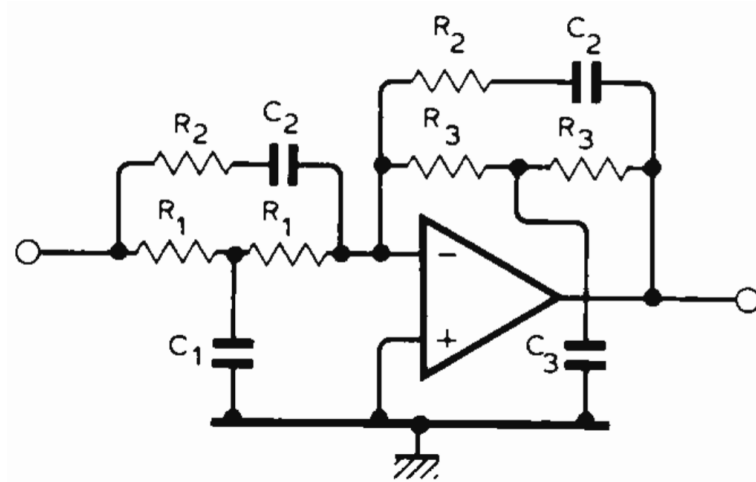
$$R_2 = 2kR_1, \tag{3.25}$$

$$R_3 = R_1 \left(\frac{f_o}{f_p}\right)^2, \tag{3.26}$$

$$C_1 = C_2 [2Q_o(1+k)]^2, \tag{3.27}$$

$$C_3 = C_1 \left(\frac{f_p}{f_o}\right)^2. \tag{3.28}$$

Since the component values given by these formulas are obviously not practical, readily available component values were used. Namely: $R_1 = 2.7k\Omega$, $R_2 = 10k\Omega$, $R_3 = 220k\Omega$, $C_1 = 8.2\mu F$, $C_2 = 47nF$ and $C_3 = 100nF$. Now, f_o, f_p, Q_o and Q_p will have to be calculated again to check whether they are not too much deviant from the designed values. This can be done using Equations 3.29 to 3.32 [18]:

$$f_o = \frac{1}{2\pi R_1 \sqrt{C_1 C_2}}, \tag{3.29}$$

$$f_p = \frac{1}{2\pi R_3 \sqrt{C_2 C_3}}, \tag{3.30}$$

$$Q_o = \frac{R_1}{2R_1 + R_2} \sqrt{\frac{C_1}{C_2}}, \tag{3.31}$$

$$Q_p = \frac{R_3}{2R_3 + R_2} \sqrt{\frac{C_3}{C_2}}. \tag{3.32}$$

$$\tag{3.33}$$

Now, using the component values above, the frequencies and Q-factors become: $f_o = 95Hz$, $Q_o = 2.3$, $f_p = 10.55Hz$ and $Q_p = 0.71$, which are quite accurate. Finally, the circuit with the calculated component values was simulated in PSpice, of which the result can be seen in Figure 3.26. This result closely matches that of the ideal theoretical version, which means the analogue design of the Linkwitz transform is successful. The bode plot of the system using both the PI controller and Linkwitz Transform is shown in Figure 3.27. At $20Hz$, the deviation from $0dB$ is $-0.007dB$, which is an improvement over the original $-23dB$ of the plant of $-22.993dB$. Here can be seen that the problems that arose when K_p was changed from $K_p = 1$ to $K_p = 25$ are partly suppressed. However, the error of $-0.17dB$ fater $200Hz$ is still present. Since the loudspeaker itself works better at the frequencies where this error is present, coupled with the fact that the plant estimation is only reliable in the range of $10Hz \leq f \leq 400Hz$, suggests that the controller should be disabled outside of the required bandwidth. This will be discussed in more detail in Section 3.2.4.

3.2.3. Adders and Subtractors
Additional analogue adders and subtractors are needed to realise the complete system. The subtractor is needed to realise the comparison of the input with the sensor output. Adders may possibly be used later on. The adder circuit is illustrated below in Figure 3.28. The output of this circuit can easily be determined using nodal analysis. The result is as required as can be seen in Equation 3.34.

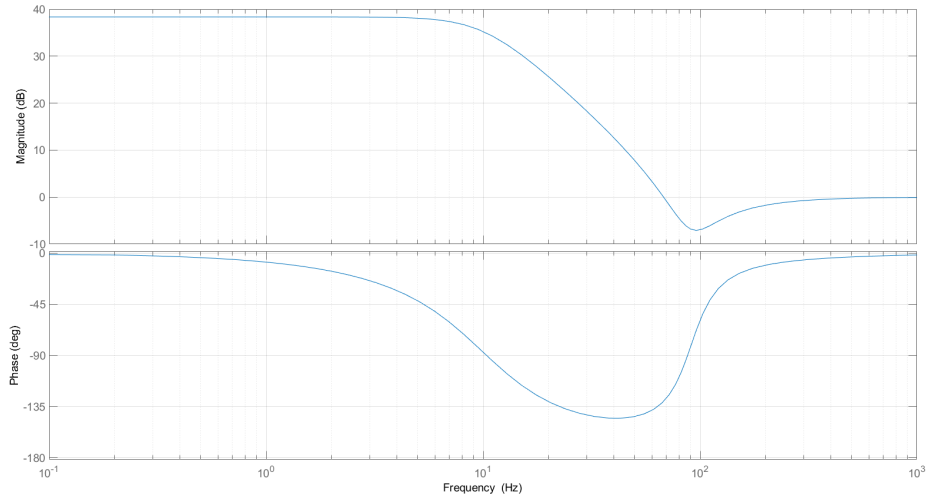$$V_o = \frac{R_{af}}{R_{a1}} \cdot V_1 + \frac{R_{af}}{R_{a2}} \cdot V_2. \tag{3.34}$$

Figure 3.25: The bode plot of the ideal theoretical Linkwitz transform.
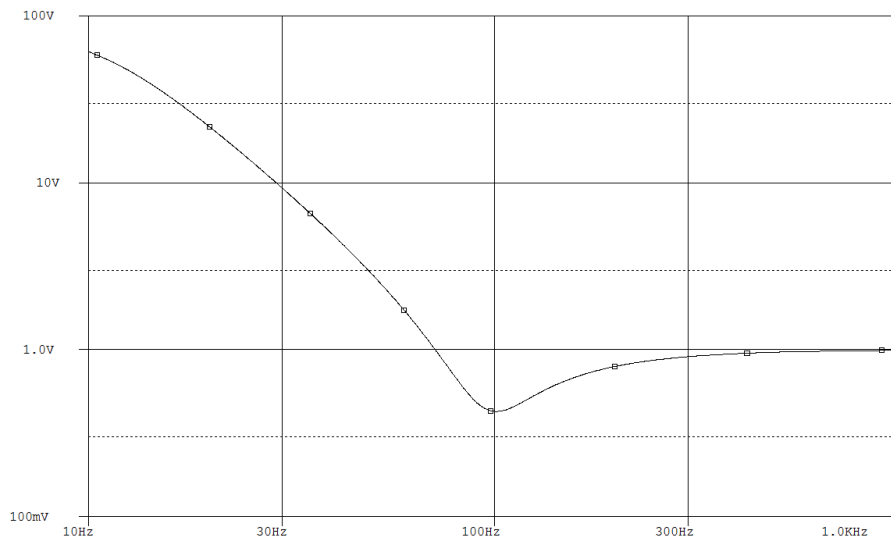

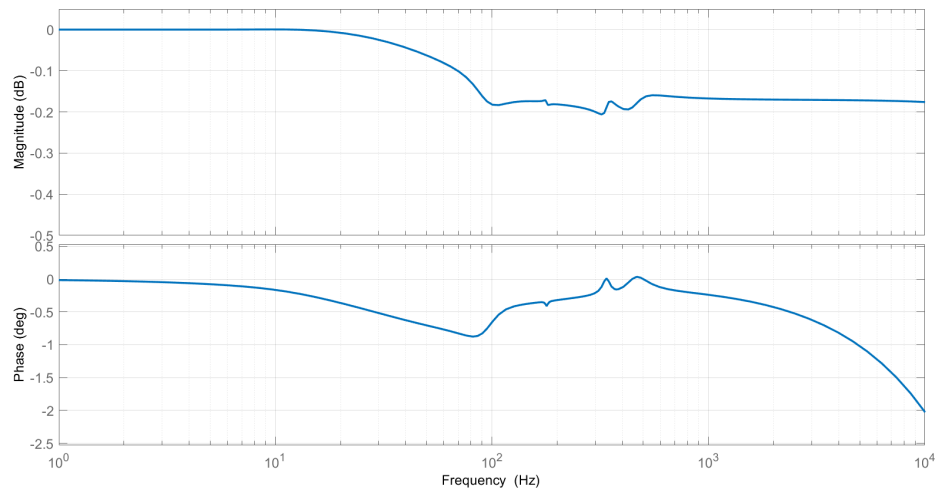Figure 3.26: The simulations of the Linkwitz transform in Pspice.

Figure 3.27: The controlled system when including the Linkwitz transform. Now with a minimum of $-0.205dB$ at $321Hz$.
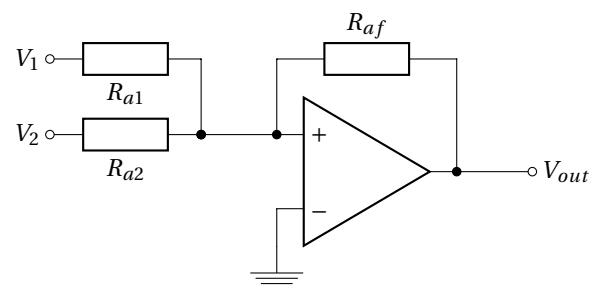

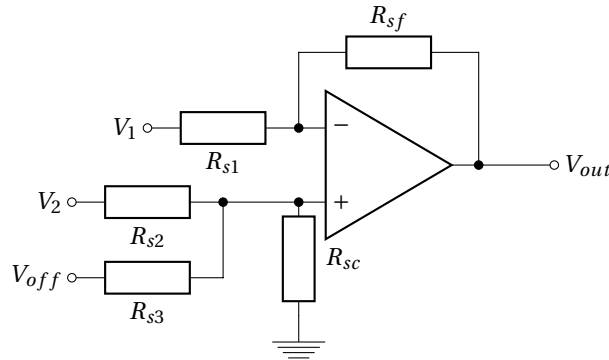Figure 3.28: A schematic view of the adder circuit.

Figure 3.29: A schematic view of the subtractor circuit.

While this adder circuit is not needed yet for implementing the controller, it might be necessary when additional filters are implemented in the system. These additional filters are described in Section 3.2.4. The subtractor circuit can be seen in Figure 3.29 The output can easily be derived through nodal analysis. In an ideal situation, the output of the subtractor would be:

$$V_{out} = V_2 + V_{off} - V_1, \tag{3.35}$$

where V_2 would be the input signal, V_1 would be the accelerometer output and V_{off} is the induced offset which was described in Section 3.2.1.1.

3.2.4. Filters

The final components to be designed are the additional filters, to make the system function correctly. Two different types of filters are needed in the system. First a filter is needed for the accelerometer, and secondly, filters are needed to disable the controller for high frequencies. An important design consideration is the fact that adding filters might make the system unstable. This will be discussed in more detail in the next two sections.

3.2.4.1. Accelerometer Offset Filter

First the accelerometer filter is considered. The accelerometer output has an offset of about $6V$, which, if untreated, could results in a wrong error signal. This causes the controller to fail, as this offset will be added to the offset created in the controller, causing clipping before the offset can be removed by filters. This means the offset will have to be removed before the feedback signal is subtracted from the input signal. This can be achieved by using a high-pass filter with a low enough cut-off frequency such that the signal is not influenced by this filter. Thus a cutoff frequency of $f_c = 1Hz$ is used. Before moving on, the stability of the system will have to be re-verified, as the phase margin will decrease. A pole-zero plot has been made for first, second and fourth order Butterworth filters, which can be seen in Figures 3.30, 3.31 and 3.32. Here can be seen that a first order and second order filters are stable, as it does not have any poles to the right of the imaginary axis. Since a first order filter would be sufficient, this was used. Since an audio capacitor of $C = 3.9\mu F$ was available, this was used, which means the resistor had a value of $R = 40k\Omega$ was used. Lastly, also a voltage follower was added to make sure the filter does not have any influence on the subtractor.

3.2.4.2. Disabling Filters

The second type of filters are the disabling filters, which have the purpose of shutting off the controller for frequencies above $f = 300Hz$. This is because of two reasons. Firstly, the accelerometer has a resonance peak of its own at around $f = 2kHz$, after which the output signal is not useful anymore. This resonance peak has to be outside the frequency range in which the accelerometer is used. Secondly, the system performs better at high frequencies, and the distortions are harder to remove using motional feedback. Also the controller becomes less reliable at higher frequencies, as it has been designed for the frequency range $10Hz \leq f \leq 400Hz$, which means its functionality cannot be guaranteed. Also, the loudspeaker should

Figure 3.30: The pole-zero plot of the system with a offset removing first order high-pass filter in the feedback loop. There is also a pole present outside of the view at $-1.78 \cdot 10^{6}$

Figure 3.31: The pole-zero plot of the system with a offset removing second order high-pass filter in the feedback loop. There is also a pole present outside of the view at $-1.78 \cdot 10^{6}$
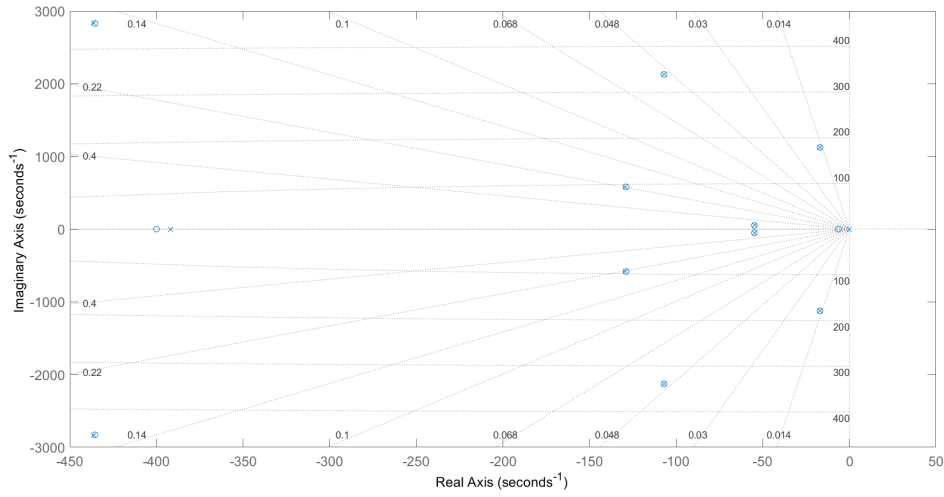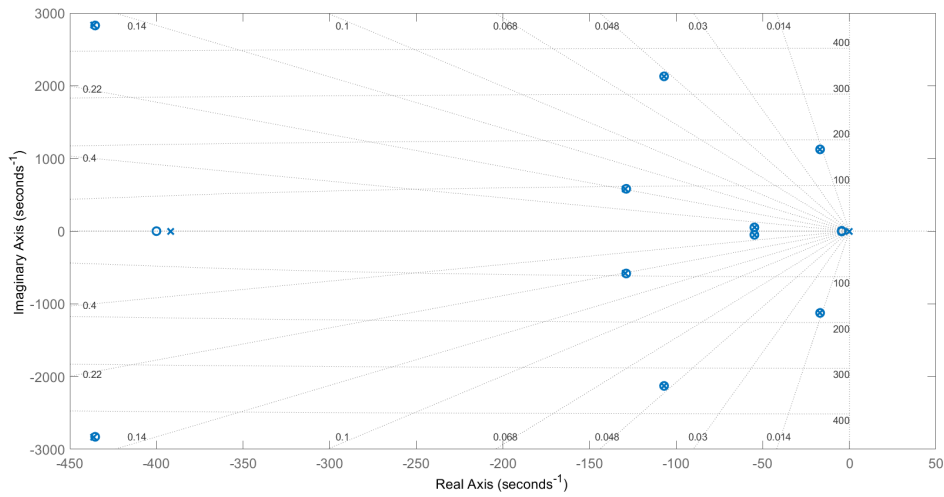
Figure 3.32: The pole-zero plot of the system with a offset removing fourth order high-pass filter in the feedback loop. There is also a pole present outside of the view at $-1.78 \cdot 10^6$

still be able to output a signal, which means an alternative path should be added for the frequencies above $f = 300Hz$. The topology of such a system including the filters is depicted in Figure 3.33. Essentially three filters are added. The first is to limit the frequencies of the output of the accelerometer to $f < 300Hz$, as above this frequency the output becomes unreliable. The second filter is used to disable the controller, as the output becomes useless when no feedback signal is present, meaning the system will fail. This filter was already shown in Figure 3.22 when discussing the controller. The last filter to be added is a high-pass filter to provide a secondary path for frequencies above $300Hz$. Notable is that another adder is necessary to converge the two paths. Also the adder can be placed after the Linkwitz transform, as this only has a benefit for low frequencies. The stability of this system will have to be checked as well. From the results of the previous section, only first-order filters were considered. The pole-zero plot for this can be seen in Figure 3.34. From this, it can be seen that the system is stable when these three filters are added. The stability of the system when combining these filters with the offset filter also has to be checked. The pole-zero plot for this can be seen in Figure 3.35. Still, the system is stable, which means all the necessary components can be constructed and assembled together. However, an additional peak is induced by adding these filters, which can be seen in Figure 3.36, in which the response of the total system can be seen. This peak is caused by the low-pass filter in the feedback loop. However, this filter is actually not needed for the system to function correctly, thus it can be left out. The response of the final system can then be seen in Figure 3.37. Now at $20Hz$, the deviation is $+0.05dB$, which is a small improvement over the system with only a controller and a Linkwitz transform. This means that the linear distortion has been reduced by 99.88%. Also the system has a bandwidth of $1Hz \leq f \leq 12.9kHz$. However, this is inaccurate because of the plant was estimated in the range $10Hz \leq f \leq 400Hz$. This means that only this range can be theoretically guaranteed.
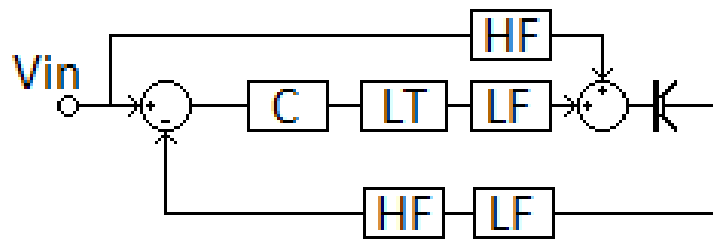
Figure 3.33: A schematic view of the total system, which includes the three disabling filters and the first order offset removing high-pass filter. C is the controller, LT is the Linkwitz transform and LF and HF are low- and high-pass filters
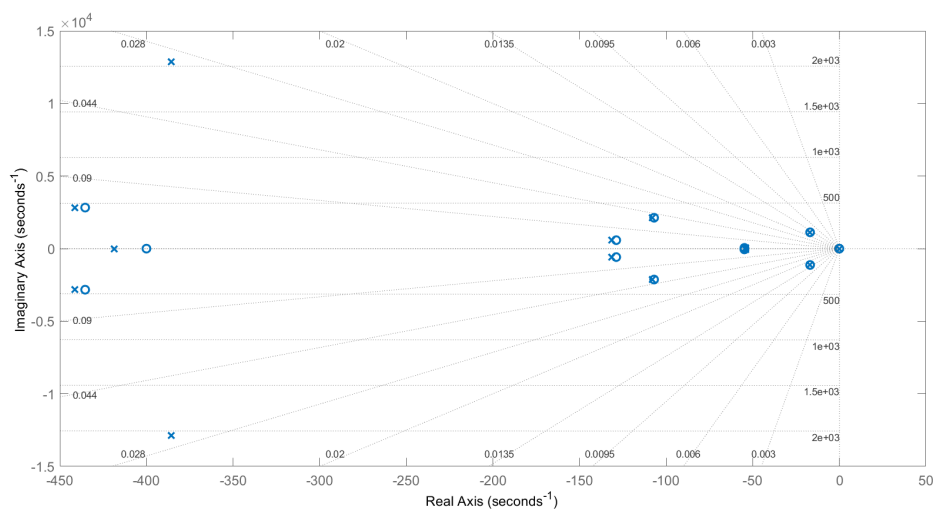

Figure 3.34: The pole-zero plot of the system when using the three disabling filters. A pole at $-3.61 \cdot 10^4$ and a zero at $-4.66 \cdot 10^4$ are out of view
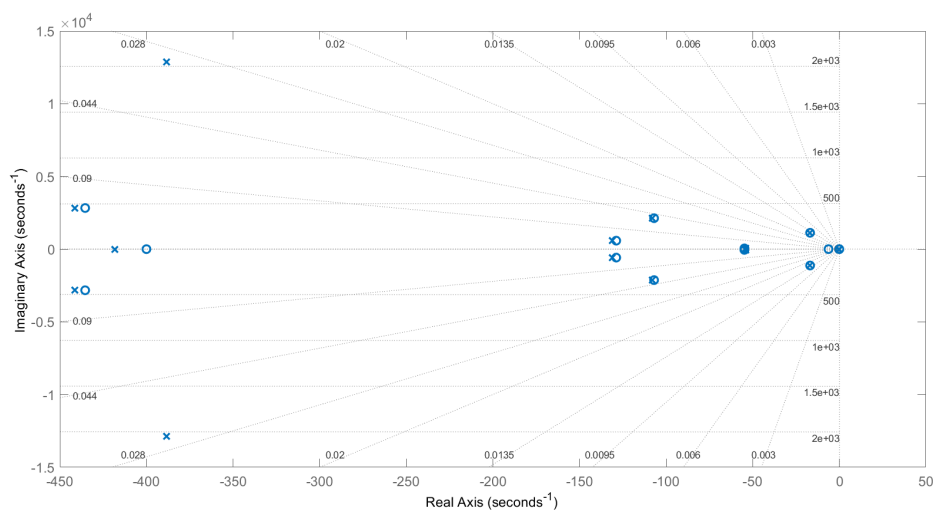

Figure 3.35: The pole-zero plot of the system when using the three disabling filters and the first order offset removing high-pass filter. A pole at $-3.61 \cdot 10^4$ and a zero at $-4.66 \cdot 10^4$ are out of view
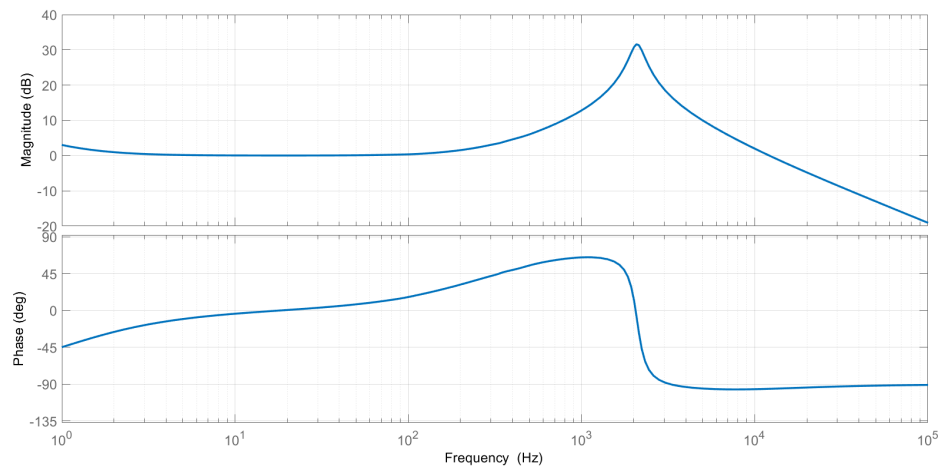
Figure 3.36: The Bode plot of the complete system including the two types of filters.
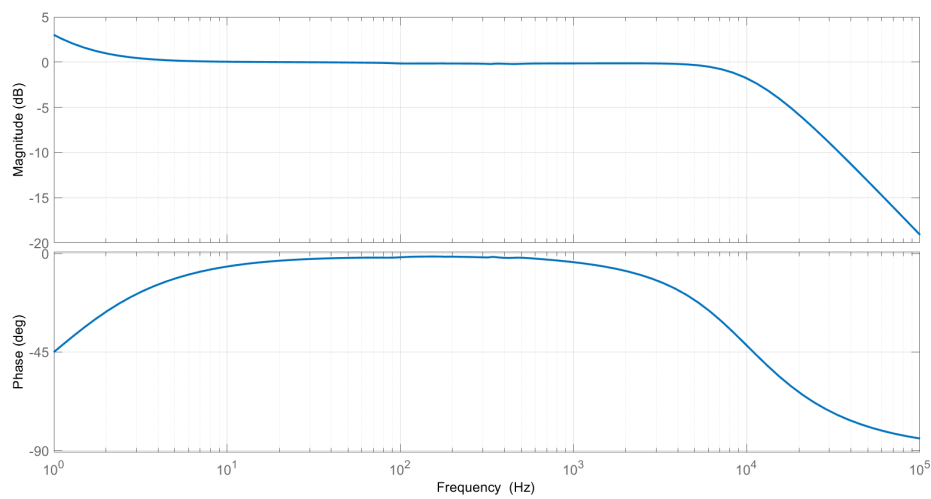

Figure 3.37: The Bode plot of the complete system including the two types of filters, with the exception of the low-pass filter in the feedback.

4

Testing

Testing of the built prototype needs a well structured measurement plan to guarantee sensible results. It simply breaks down to testing the main sub-components of the system separately after which the whole system is tested if each module functions as required. The tests will first be conducted using a measurement setup consisting of the circuit, a function generator, oscilloscope and DC voltage sources. In the subsequent sections more will be elaborated on what is expected from the prototype, the measurement plan and corresponding measurement setup and the measurement results. The interpretation of the obtained results will be more comprehensively discussed in Section 5.

4.1. Prototype Expectations

The controller consists of the following components:

1. A PI-module with pre-amplifier.

2. A Feedback high pass filter.

3. An Output high pass filter.

4. A Subtractor

The complete PI-controller as mentioned previously can be expressed as $K_p + K_i \cdot \frac{1}{s}$, were $K_p = 23$ and $K_i = 9583$. These values are slightly different from the ideal values, as the used component values are slightly different from the ideal values. The PI-controller is also operational at lower frequencies, which means that the integrated signal will be more dominant at the output due to the its high gain. Previously was mentioned that due to the high DC voltage gain of the PI-controller part the input offset voltages where immensely amplified, which caused clipping. The pre-amplifier was added before the integrator to gradually increase the gain of the error signal and reject the offset preventing clipping from happening. Another high pass filter was added at the output to fully remove the offset.

From each individual component the following is expected:

1. The Proportional-integral module: integration of the error signal is expected without any sign of clipping or other forms of distortion. There will possibly be some small offset at the output. Since the majority of the input signals will be constructed of sines, amplified cosines are expected at the output with a small ripple of amplified sines.

2. Subtractor: it is simply expected to correctly subtract the input signals.

3. Output high pass filter: integrated error signal with minimum offset.

4. Feedback high pass filter: removal of the accelerometer offset.

5. Pre-amplifier: Due to the addition of a capacitor to ground it is expected that sine waves will be amplified properly, but offset voltages will not be amplified. Bias current however may impose some offset at the output, but it is expected to not be high enough to cause clipping.

4.2. Measurement Plan

The previous section subtly indicates that the testing of the prototype has taken place in stages in a specific order i.e each individual element will be tested in the right order. To prevent causing damage to the loudspeaker and other equipment, testing was first done by manually delivering and adjusting representative input signals to the prototype. If and only if promising results are obtained, the system will be tested using the speaker. The testing has only been done on the system consisting of the system without the Linkwitz module, since it still needs to be built. Also due to the limited amount of time it seems unrealistic for the system, or at least some part of it, to be tested using the loudspeaker. In short tests have been conducted only on the prototype without the Linkwitz module by using voltage sources, function generators and oscilloscopes.

Testing the whole system will be done in the following stages:

1. First the high pass filter in the feedback loop will be tested by giving an sine wave on top of an offset voltage at its input using a function generator. If the offset is reduces without affecting the sine wave, the filter operates properly. The voltage follower after the filter will prevent the filter from affecting the subtractor.

2. After the feedback filter the subtractor will be tested. Several signals generated by the function generator will be fed to the inputs of the subtractor with various amplitudes and frequencies. Determining whether or not the output is as required will require careful observation of the results on the oscilloscope.

3. With the same signals fed to the feedback filter and the subtractor inputs, the output of the pre-amplifier will be measured. There will be checked whether, if there is any, offset is rejected and the signal is amplified with no distortion. It is very important the there is very little offset at the input of the integrator.

4. The proportional-integral module will be tested. The additional capacitor to ground will cause the offset not to be amplified. At the output of the PI-module will be checked whether the error signal is integrated and whether the offset is rejected. To ensure that all offset is rejected another high pass filter is added after the PI-module. This will be tested at the end.

4.3. Measurement Results

Due to time constraints the PI-controller was tested directly for now, skipping the testing of the individual modules. Fortunately, the system functions as expected. At the positive input of the subtractor four test signals were fed, namely: 20 Hz, 50 Hz, 100 Hz and 300 Hz. The 20 and 100 Hz signals where chosen, because these are at the boundary of the controller frequency range. The results are illustrated in Figures 4.1, 4.2, 4.3 and 4.4, where yellow represents the input signal and blue the output.

Also needs to be said that during testing the PI-controller was no working at first due to the polar capacitor of high pass filter at the output. The capacitor and resistor were than replaced, but still holding the same cut-off frequency. The test where then conducted successfully.

The peak-to-peak values and mean values were measured of the different situations listed in Table 4.1. For the interpretation see Section 5.
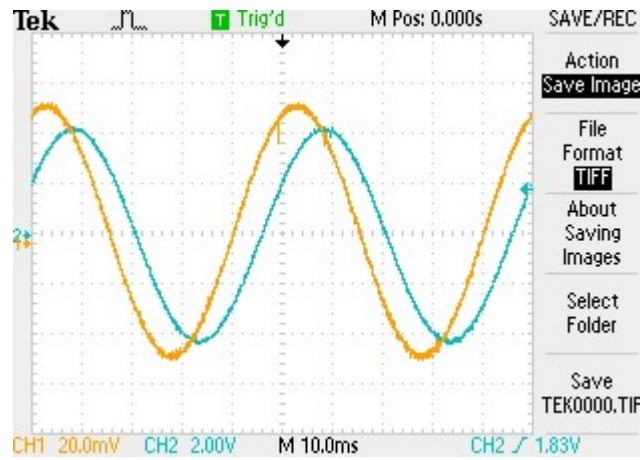
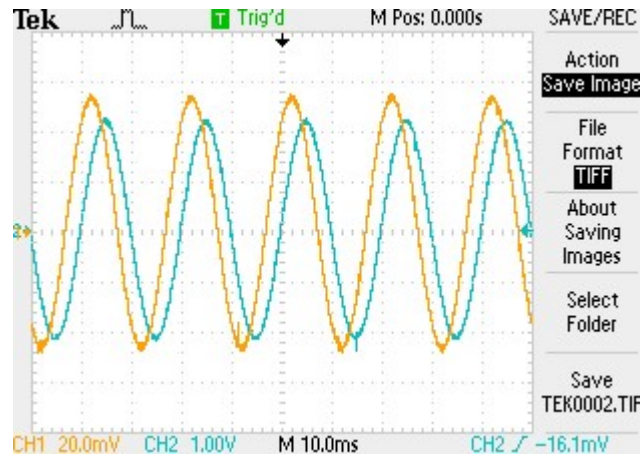Figure 4.1: PI-controller output (blue) of 20 Hz input signal (yellow)

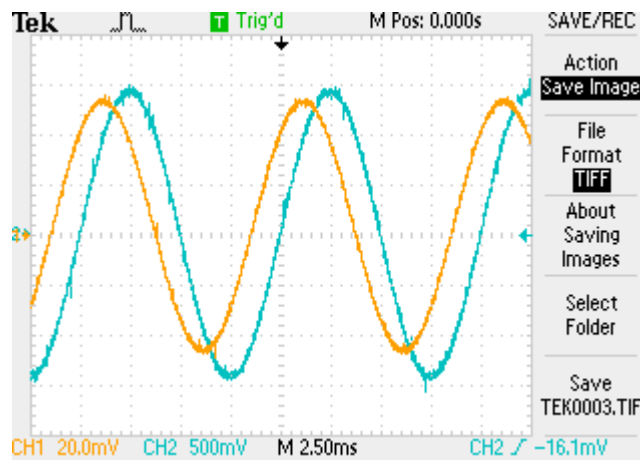Figure 4.2: PI-controller output (blue) of 50 Hz input signal (yellow)

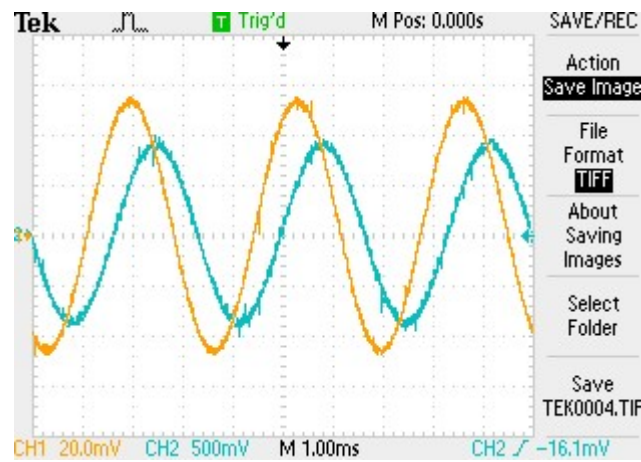Figure 4.3: PI-controller output (blue) of 100 Hz input signal (yellow)

Figure 4.4: PI-controller output (blue) of 300 Hz input signal (yellow)

Table 4.1: System measurements

Frequency [Hz]	Input Voltage [mV]	Output Voltage[V]	Gain	Mean Input [mV]	Mean Output [mV]
20	103	8.72	84.66	3.43	10.30
50	105	4.60	43.81	3.80	2.22
100	104	3.02	29.04	-0.439	10,9
300	110	2.00	18.18	3.88	-3.54

4.4. Future measurements

Currently, only tests have been conducted on the PI-controller. Implementing the Linkwitz filter still needs to be done, after which it will be tested. Also a measurement plan and setup needs to be made. This will most likely be finished in the week of the thesis deadline, which will hopefully lead to testing the complete prototype.

5

Discussion

The results from Section 4 are illustrated quite abstractly of which interpretation will be provided. Also whether or not the steps taken during the design process, the testing period, and the performance of the team was adequate or not will be be assessed by means of a reflection. Lastly, recommendations for future work will be enlisted.

5.1. Interpretation

Due to the limited time a short test was done on the PI-controller. By directly testing the output of this system and analysing whether the results are as required it could be quickly known whether or not it works. Luckily the test results did show the expected behaviour. This will of course be tested more extensive and assessed critically. But by only looking at the results obtained in the previous section the following can be concluded:

1. The input signal is amplified more at lower frequencies than higher frequencies, as would be expected from an integrator.

2. The signals at the output were also phase shifted by approximately 90 degrees i.e. sines are being integrated into cosines.

3. The offset is successfully rejected as can be seen in Section 4 in Table 4.1 by looking at the mean values of the output.

The characteristics mentioned above for now show integrator behaviour. Since the signal which is amplified is quite small relative to the integrated signal, it cannot easily be seen.

5.2. Reflection

A brief reflection will be given on the way the sub-group operated during the design process. Even though the design process took place quite structured, some important individual task were executed wrongly. Using the wrong method to estimate the frequency response was one of the big mistakes, which caused us quite some time to cover for it. Eventually the estimation capabilities of the System Identification Toolbox was used to estimate the correct frequency response. During the prototyping process of the PI-controller the circuit was rebuilt several times due to the clipping problem we identified caused by offset voltages at the input of the op amp. The circuit wasn't simulated properly by not taking the offsets into account, this lead us to believe that nothing was wrong with the simulated circuit. After simulating the circuit properly by modelling the non-idealities of the op amps, we discovered that even the smallest offset at the input was magnified tremendously by the gain of the PI-controller. At this point it took very little time to realise that the gain of the PI-controller needed to be added in stages, which did solve the problem.

There were also some good characteristics in the group in terms of teamwork, planning and trying to solve problems as independent as possible and teamwork. Even though several problems did occur costing time,

we did manage to produce a working PI-controller before the thesis deadline. The whole group in general also emitted good overall teamwork by helping other sub-groups when needed.

6

Conclusion

Unfortunately, as no measurements of the controller on the plant have been done, due to time constraints, no solid conclusion can be made about the suppression of nonlinear distortion. This is because the plant model used to design the controller was only linear, which means that not even theoretically a quantitative prediction can be made. The only prediction that can be made is that the nonlinear distortion will be suppressed partially because of the loop gain, but how much will have to be measured. A better conclusion can be made on the linear distortion and the MFB bandwidth, even though no measurements were conducted. Firstly, at $20Hz$, the output of the plant was $-23dB$, after implementation of the controller, Linkwitz transform and filters, the output of the system became $+0.005dB$. This means the linear distortion of the plant was reduced by 99.88%. Secondly, the bandwidth in theory also meets the requirement of being at least in the range of $10Hz \leq f \leq 300Hz$. This fact has been seen in Section 3. The theoretical bandwidth was $1Hz \leq f \leq 1.29kHz$. This cannot be guaranteed, however, as the plant estimation is only accurate in the range $10Hz \leq f \leq 400Hz$. Nothing about achieving the rest of the requirements can be said just yet, however. This is because only a prototype has been built, which does not include the Linkwitz transform. This means no cost, power usage, THD reduction and volume of the system can be identified yet. The Signal to Noise ratio of the system also will still have to be measured when its fully assembled and tested, which means no sensible conclusion can be made on that as well.

Finally, a few things will have to be finished before a complete conclusion can be made on this project. Firstly, the effect on the controller on its self will have to be tested on the system. Then the Linkwitz transform and the filters will have to be added, and the THD will have to be measured, as well as the signal to noise ratio and the power consumption. Finally, the cost of the individual components, and a possible PCB, are to be calculated. As still two weeks are left, this can probably be achieved.
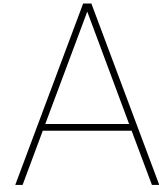
A
Appendix

A.1. Matlab Script

```matlab
% ---------- System Estimation ----------------
% Opening The Amplitude Response and Saving the Data
fig = openfig('amplitude4_vol85_gitaar.fig');
ampl_fig = findobj(gca,'Type','line');
Freq = get(ampl_fig,'Xdata');
Ampl_dB = get(ampl_fig,'Ydata');

% Opening The Phase Response and Saving the Data
fig2 = openfig('phase4.fig');
angle_fig = findobj(gca,'Type','line');
Theta = get(angle_fig,'Ydata');

% Calculation of the Response
Ampl = 10.^(Ampl_dB/20); % Convert the Amplitude from dBW to V
Response = Ampl .* exp(1i * Theta * pi/180); % Calculating the
    Response
Responsee = Response(219:8739); % Limiting the Response between 10 Hz
    - 400 Hz
Freqe = Freq(219:8739)'; % Limiting the frequencies between 10 Hz -
    400 Hz
Freqe_w = 2 * pi * Freqe; % Converting from Hz to rad/s

% Setting up an Estimation Object
BW = 10e3;
Ts = 1/(2*BW);
gfre = idfrd(Responsee, Freqe_w, Ts);

% Choosing Estimation Options
tfest_opt = tfestOptions;
tfest_opt.EnforceStability = true;
tfest_opt.Display = 'on';
tfest_opt.SearchOption.MaxIter = 40;
tfest_opt.SearchOption.Tolerance = 1e-30;

% A Ninth-order Estimation of the Plant
```

```
33  syse_9 = tfest(gfre, 9, tfest_opt);

34
35  % % Checking for Stability
36  % rlocus(syse_9);

37

38
39  % --------- Calculating the Maximum Input Voltage
40  Vamp_max = 0.75;
41  Vpp_max = 1.5;
42  Amplification = 1./(abs(Responsee));
43  Max_Amp = Vamp_max./Amplification;
44  % semilogx(Freqe,Max_Amp)
45  % loglog(Freqe,Max_Amp)

46

47
48  % --------- Controller -------------
49  % PID Parameters
50  Kp = 25;
51  Ki = 10000;
52  Kd = 0;
53  C = pid(Kp, Ki, Kd, 0); % PID controller

54

55
56  % ------- Linkwitz Transform -------
57  fo = 91; % Resonance Frequency of the Loudspeaker
58  fp = 10; % Desired Cut-off Frequency
59  qo = 2.2; % Q-Factor at the Resonance Frequency
60  qp = 0.707; % Desired Q-factor

61
62  % The Theoretical Transfer Function
63  LWT = (s^2+2*pi*fo*s/qo+(2*pi*fo)^2)/(s^2+2*pi*fp*s/qp+(2*pi*fp)^2);

64
65  % This Needs to be More Than 0 for Feasible Implementation
66  k = (fo/fp-qo/qp)/(qo/qp-fp/fo);

67
68  % Calculating the Component Values
69  CL2 = 47e-9;
70  RL1 = 1/(2*pi*fo*CL2*(2*qo*(1+k)));
71  RL2 = 2*k*RL1;
72  CL1 = CL2 * (2*qo*(1+k))^2;
73  CL3 = CL1 * (fp/fo)^2;
74  RL3 = RL1*(fo/fp)^2;

75
76  % Checking for Correct Functioning
77  % Actual Used Values
78  RL1 = 2.7e3;
79  RL2 = 10e3;
80  RL3 = 2.2e5;
81  CL1 = 8.2e-6;
82  CL2 = 47e-9;
83  CL3 = 10e-8;

84
85  % These Need to be Approximately Equal
86  fp1 = 1/(pi*CL1*RL1);
```

```matlab
87  fz1 = 1/( pi*CL3*RL3 ) ;
88
89  % These Will Need to Match the Previously Chosen Values For Fo, Qo, Fz
        , Qz
90  fot = 1/(2*pi*RL1*sqrt(CL1*CL2)) ;
91  fpt = 1/(2*pi*RL3*sqrt(CL2*CL3)) ;
92  qot = RL1/(2*RL1+RL2)*sqrt(CL1/CL2) ;
93  qpt = RL3/(2*RL3+RL2)*sqrt(CL3/CL2) ;
94
95
96  % --------- Filters ----------------
97  fh = 1; % Cutoff Frequency for the Offset Removal Filter
98  fc = 300; % Cutoff Frequency for the Disabling Filters
99
100 % Setting up the Transfer Functions of the Filters
101 % Transfer Function Parameters
102
103 % Offset Removal Filters
104 [b11h, a11h] = butter(1,2*pi*fh,'high','s'); % First Order Filter
105 [b21h, a21h] = butter(2,2*pi*fh,'high','s'); % Second Order Filter
106 [b41h, a41h] = butter(4,2*pi*fh,'high','s'); % Fourth Order Filter
107
108 % Disabling Filters
109 [b1,a1] = butter(1,2*pi*fc,'s'); % Low Pass Disabling Filter
110 [b1h,a1h] = butter(1,2*pi*fc,'high','s'); % High Pass Disabling Filter
111
112 % Constructing the Transfer Functions
113 F11_h = tf(b11h,a11h); % First Order Offset Removal Filter
114 F21_h = tf(b21h,a21h); % Second Order Offset Removal Filter
115 F41_h = tf(b41h,a41h); % Fourth Order Offset Removal Filter
116 F1_h = tf(b1h,a1h); % Low Pass Disabling Filter
117 F1 = tf(b1,a1); % High Pass Disabling Filter
118
119 % % Checking For Stability
120 % % Only with Offset Removal Filter
121 % Closed_Loop = feedback(C*LWT*syse_9,F11_h); % First Order Check
122 % Closed_Loop = feedback(C*LWT*syse_9,F21_h); % Second Order Check
123 % Closed_Loop = feedback(C*LWT*syse_9,F41_h); % Fourth Order Check
124 %
125 % % Only With Disabling Filters
126 % Closed_Loop = feedback((F1*C*LWT+F1_h)*syse_9,F1);
127 %
128 % % Both Types of Filters Combined
129 % Closed_Loop = feedback((F1*C*LWT+F1_h)*syse_9,F11_h);
130 %
131 % pzmap(Closed_Loop);
```

Bibliography

[1] Y. Li and G. T. C. Chiu, "Control of loudspeakers using disturbance-observer-type velocity estimation," *IEEE/ASME Transactions on Mechatronics*, vol. 10, no. 1, pp. 111–117, February 2005.

[2] C. G. C. C.-C. P. H. Chen, C-Y, "Passive voice coil feedback control of closed-box subwoofer systems," *Journal of Acoustical Society of AmericProceedings of The Institution of Mechanical Engineers Part C-journal of Mechanical Engineering Science*, vol. 214, no. 7, pp. 995–1005, July 2000.

[3] J. Klaassen and S. de Koning, "Motional feedback with loudspeakers," *Phillips Technical Review*, vol. 29, no. 5, pp. 148–157, 1968.

[4] I. Forgusson. (2010, May) Loudspeaker cross section. [Online]. Available: http://en.wikipedia.org/wiki/File:Speaker-cross-section.svg

[5] C. Sean, "A direct pwm loudspeaker feedback system," Master's thesis, Massachusetts Institute of Technlogy, 1996.

[6] J. V. s. Lawrence E. Kinsler, Austin R. Frey, *Fundementals of Acoustics*, 4th ed. John Wiley & Sons, Inc., 2000.

[7] W. Klippel, "Loudspeaker nonlinearities - causes, parameters, symptoms." *Journal of Audio Engineering Society*, vol. 54, no. 10, pp. 907–939, October 2006.

[8] K. M. Al-Ali, "Loudspeakers: Modeling and control," Ph.D. dissertation, University of California at Berkeley, 1999.

[9] Jakobsson and M. D. Larsson, "Modelling and compensation of nonlinear loudspeakers,," Master's thesis, Chalmers University of Technology, 2010.

[10] R. Valk, "Control of voicecoil transducers," Master's thesis, Delft University of Technology, 2013.

[11] R. Hilmisson, "Feedback linearisation of low frequency loudspeakers," Master's thesis, Technical University of Denmark, sep 2009.

[12] J. Elliot. (2016, sep) Philips motional feedback speakers. [Online]. Available: http://hifipig.com/philips-motional-feedback-speakers/

[13] D. D. greef and J. Vandewege, "Acceleration feedback loudspeaker," *wireless world*, 1981.

[14] Philips, "Philips sonant," *Elektor*, vol. 122, pp. 216–219, sep 1975.

[15] W. B. Tijs Hol, "Digital control in a motional feedback audio system," Delft University of Technology, Tech. Rep., 2016.

[16] T. E. Marlin, *Process Control. Designing Processes and Control Systems for Dynamic Performance*, 2nd ed. McGraw-Hill, 1995, chapter15: Feedforward Control.

[17] S. Linkwitz, "Loudspeaker system design: A three-enclosue loudspeaker system with active delay and crossover: Part 2," *Wireless World*, vol. 84, no. 1510, pp. 67–72, jun 1978.

[18] ——, "Loudspeaker system design: Changes and refinements to the system described in the may and june issues," *Wireless World*, vol. 84, no. 1516, pp. 79–83, dec 1978.

[19] ——. (2018, jun) Active filters. [Online]. Available: http://www.linkwitzlab.com/filters.htm

[20] G. Franklin, J. Powell, and A. Emami-Naeni, *Feedback Control of Dynamic Systems*, 7th ed. Pearson, 2014.

[21] SilverStar. (2006, oct) Depicts a traditional pid controller. [Online]. Available: https: //en.wikipedia.org/wiki/File:Pid-feedback-nct-int-correct.png

[22] S. W. Sung and I.-B. Lee, "Limitations and countermeasures of pid controllers," *Ind. Eng. Chem. Res.*, vol. 35, no. 8, pp. 2596–2610, 1996.

[23] G. Janssen, J. Creemer, D. Djairam, M. Gibescu, I. Lager, N. van der Meijs, S. Vollebregt, R. Roodenburg, J. Hoekstra, and X. van Rijnsoever, *Student Manual - Lab Course EE Semester 1*, Technische Universiteit Delft, 2015 - 2016.

[24] (2018, May) Transfer function estimation - matlab tfest- mathworks benelux. [Online]. Available: https://nl.mathworks.com/help/ident/ref/tfest.html